Development of a Reconfigurable Multi-Material Polymer Based-Extrusion System

by

David Moises Baca Lopez

A thesis submitted in partial fulfillment of the requirements for the degree of

Master of Science

in

Engineering Management

Department of Mechanical Engineering

University of Alberta

Abstract

Fused deposition modelling has become one of the most prominent additive manufacturing processes for the fabrication of thermoplastic polymers. It is generally used for rapid prototyping and industrial batch production, and due to its capabilities to fabricate a wide range of materials, FDM is gaining high popularity, especially for producing complex geometries using multi-material 3D printing. Extensive research has been done on optimizing and improving the mechanical properties of thermoplastic materials, but its relationship linking the equipment itself with multi-materials and part designs leads to a gap between different stages of this extrusion technology. From this viewpoint, this thesis focuses on the FDM technique and presents a system developed at the Laboratory of Intelligent Manufacturing, Design, and Automation (LIMDA) for multiple material thermoplastic polymers. The system is capable of depositing in any given layer or geometry, up to three different types of materials. This system is intended to handle a variety of multi-material print head nozzles based on the AM process requirement. Multi-material 3D printing and process parameters optimization using multiple extruders are considered one of the main challenges for the FDM technique; therefore, a comparison of two modes: multi-material single mixing nozzle and multi-material

multiple nozzles, linking the technology with the mechanical properties is presented. Tensile testing specimens were printed in two different scenarios to validate the comparison: (1) multi-material multi-layered section printed using a multi in-out single mixing nozzle and (2) multi-material multi-layered section printed using a multiple extrusion nozzle within the same carriage. Both modes followed a rectilinear infill pattern and different material combinations. The material combinations implemented included ABS-HIPS, ABS-PLA, PLA- HIPS, and PLA-HIPS-ABS. A behavioural study is evaluated on the mechanical properties of these materials. The results provide a tool for selection on which type of mode is considered suitable for maximizing efficiency and performance to fabricate a multi-material 3D printed product. Besides, the mechanical properties of materials produced through FDM lack of strength, which restricts the production of high-level multi-functional components. Standard 3D printing materials are typically used for conceptual parts rather than functional parts. The fabrication of a specimen with a sandwich material combination using PLA, ABS, and HIPS through the filament-based extrusion process can demonstrate an improvement in its properties. This thesis also aims to assess among these common thermoplastic materials, the best material sandwich-structured arrangement design, to enhance the mechanical properties of a part and to compare the results with the homogeneous materials selected. The samples were

subjected to tensile testing to identify the tensile strength, elongation at break, and Young's modulus of each material combination. The experimental results demonstrate that applying the PLA-ABS-PLA sandwich arrangement leads to the best mechanical properties between these material combinations. This study enables users to consider sandwich structure designs as an alternative to manufacture multi-material components using conventional and low-cost materials. For the outcome of this research, a summary of six chapters is presented.

Preface

This thesis is an original work by David Moises Baca Lopez, and the research is performed under the supervision of Dr. Rafiq Ahmad. The development of an additive manufacturing system is presented, and two journal papers related to this thesis have been submitted or published and are listed below. As such, the thesis is organized as a combination of a traditional and paper-based thesis.

1. **David Baca,** Rafiq Ahmad*, "The impact on the mechanical properties of multi-material polymers fabricated with a single mixing nozzle and multi-nozzle systems via fused deposition modelling." *International Journal of Advanced Manufacturing Technology.* (Under review)
2. **David Baca,** Rafiq Ahmad*, "Tensile mechanical behaviour of multi-polymer sandwich structures via fused deposition modelling." *International Journal of Advanced Manufacturing Technology.* (Under review)

Acknowledgments

The author thanks the following people:

- My supervisor, Dr. Rafiq Ahmad, for his guidance, support, and for allowing me the use of all machinery in the Laboratory of Intelligent Manufacturing, Design and Automation (LIMDA), especially in automation, additive and subtractive technologies.
- Dr. Xinming Li and Dr. Mohtada Sadrzadeh for serving as committee members in my final examination.
- The Department of Mechanical Engineering and professors who taught me relevant courses during my studies.
- The Mexican National Council for Science and Technology (CONACYT) for granting the scholarship No. reference 625788/472485 to pursue my master's degree.
- The Natural Sciences and Engineering Research Council of Canada (NSERC) for the support through RGPIN-2017-04516 project for funding the experimental setup and resources.
- My mother, Maria Elena Lopez Sesma, for always supporting me through this entire journey and being understanding about my decisions.
- My close family, including uncles, aunts, and cousins, who were always supporting me.

Table of Contents

Abstract ii
Preface v
Acknowledgments vi
Table of Contents vii
List of Tables ix
List of Figures x
List of Abbreviations xii
1 Introduction 1
1.1 Background and Motivation 1
1.2 Research Objectives 3
1.3 Scope and Limitations 4
1.4 Thesis Outline 6
2 Literature Review 8
2.1 Additive Manufacturing 8
2.1.1 The Process Chain of Additive Manufacturing 9
2.1.2 Classification of AM Processes 11
2.2 Material Extrusion Process 16
2.2.1 The FDM Process 17
2.2.2 Materials for FDM 18
2.2.3 Multi-material Additive Manufacturing 21
3 Experimental Setup & Development 25
3.1 Hardware Design 25
3.2 Electronics and Software 29
3.3 System Integration, Testing & Calibration 34
4 The impact on the mechanical properties of multi-material polymers fabricated with a single mixing nozzle and multi-nozzle systems via fused deposition modelling 37
4.1 Introduction 37
4.2 Literature Review 39
4.3 Experimental technology: multi-material extrusion nozzles 42

4.3.1 Multiple mixing single extrusion 43
4.3.2 Multiple extrusion nozzle 44
4.4 Experimental Strategy 45
4.4.1 Equipment and materials 45
4.4.2 Methodology and process parameters 47
4.5 Results and Discussion 50
4.6 Conclusion 58
5 Tensile mechanical behaviour of multi-polymer sandwich structures via fused deposition modelling 60
5.1 Introduction 60
5.2 Materials and Methodology 65
5.2.1 Process Parameters 65
5.3 Experimental 67
5.4 Results and Discussion 69
5.5 Conclusion 75
6 Conclusion 76
6.1 General conclusion 76
6.2 Research contributions 77
6.3 Research limitations 78
6.4 Proposed future research 78
References 80

List of Tables

Table 2.1 Typical properties of some FDM thermoplastic polymers, examples.....21
Table 4.1 Constant parameters for 3D printing.....48
Table 4.2 Experimental results of multi-material specimens tested using both modes.....56
Table 4.3 Comparison to select the best manufacturing process based on the final product performance between single mixing nozzle and multiple nozzle extrusion.....58
Table 5.1 Typical mechanical properties of ABS, PLA, and HIPS.....66
Table 5.2 Printing parameters.....67
Table 5.3 Results on the stress-strain response homogeneous and sandwich-structured specimens.....74

List of Figures

Figure 1.1 Thesis scope 5
Figure 1.2 Thesis layout according to the research objectives 6
Figure 2.1 The process chain on additive manufacturing; a) CAD-model, b) slicing & path planning, c) physical layers & bonding, d) physical model 9
Figure 2.2 A general overview of the decision-making AM process 10
Figure 2.3 Principle of tessellation. A semi-circle model (left) is approximated with triangular facets (right). The more triangles used, the more accurately the model can be approximated 11
Figure 2.4 Classification of additive manufacturing processes based on the aggregate form of the material according to DIN 8580, based from [2] 12
Figure 2.5 The working principle of laser sintering (left) and binder jetting (right) 13
Figure 2.6 The working principle of the sheet lamination process 13
Figure 2.7 The working principle of fused deposition modelling 14
Figure 2.8 The working principle of stereolithography 14
Figure 2.9 Schematic of the aerosol jet printing 15
Figure 2.10 Different extrusion principles 16
Figure 2.11 Schematic of the material extrusion process 17
Figure 2.12 Common thermoplastic polymers for 3D printing, based from [16], [17] 18
Figure 3.1 Assembly design of the system including the subsystem printing heads deposition a) single mixing extrusion, b) multi-nozzle extrusion 28
Figure 3.2 Architecture of the multi-material FDM system 29
Figure 3.3 Process system architecture between a) single material fabrication b) multi-material fabrications 31
Figure 3.4 LIMDA graphic user interface (GUI), conversion file and process screen 32
Figure 3.5 Commercial Interface with multi-material parts, examples 33
Figure 3.6 LIMDA software architecture 34
Figure 3.7 Rear view of the electronics and electric wiring of the system 36
Figure 4.1 Classification of FDM multi-material hot end nozzles 42
Figure 4.2 Mixing nozzle hotend (three inputs and one output) 43
Figure 4.3 Multi-nozzle extrusion (four independent nozzles) 44
Figure 4.4 Setup developed at LIMDA for single mixing nozzle and multiple nozzles for the multi-material FDM system 46
Figure 4.5 Standard specimen for tensile test, dimensions are in mm 47
Figure 4.6 Simulation of specimens fabricated with a single material and multi-material 49

Figure 4.7 Specimen ABS positioned and tested in the tensile machine 49
Figure 4.8 Defects on boundary interface (left) a) ABS-PLA, b) ABS-HIPS c) PLA-HIPS-PLA using the multiple-nozzle extrusion model.....51
Figure 4.9 Effective bonding on boundary interface (right) d) ABS-HIPS-ABS, e) HIPS-ABS-HIPS, and f) ABS-HIPS-PLA using the single mixing- nozzle extrusion model.....51
Figure 4.10 Failure of multi-material specimen a) multiple nozzles and b) single mixing nozzle.....51
Figure 4.11 Mean tensile stress of all specimen tested.....54
Figure 4.12 Mean Young's modulus of all specimen tested.....55
Figure 4.13 Mean tensile elongation at break of all the specimen tested.....55
Figure 5.1 Geometry for a typical specimen as a single material and as a sandwich structure part (three-layer section with equal thickness).....66
Figure 5.2 Standard test specimen in mm.....67
Figure 5.3 Illustration of the multi-nozzle module bottom side with the X-Y offsets (left) and isometric view (right).....68
Figure 5.4 Multi-nozzle extruder while printing ABS-HIPS-ABS specimen.....69
Figure 5.5 Mean tensile stress of all specimen tested.....70
Figure 5.6 Mean Young's modulus of all specimen tested.....71
Figure 5.7 Mean tensile elongation at break of all specimen tested.....71
Figure 5.8 Examples of tested specimens a) ABS b) PLA c) HIPS d) ABS-PLA-ABS e) ABS-HIPS-ABS f) HIPS-PLA-HIPS g) HIPS-ABS-HIPS h) PLA-ABS-PLA i) PLA-HIPS-PLA.....72
Figure 5.9 Detail view of fractured specimens printed as a sandwich structure a) ABS-HIPS-ABS b) ABS-PLA-ABS c) PLA-HIPS-PLA d) PLA-ABS-PLA e) HIPS-ABS-HIPS f) HIPS-PLA-HIPS.....72
Figure 5.10 Stress-strain curve diagram of all the specimens tested.....74
Figure 6.1 Future research path.....79

List of Abbreviations

3DP	Three-Dimensional Printing
ABS	Acrylonitrile Butadiene Polystyrene
AM	Additive Manufacturing
ASCII	American Standard Code For Information Interchange
ASTM	American Society For Testing And Materials
CAD	Computer-Aided Design
CFRP	Carbon Fiber Reinforced Plastics
CFRP	Carbon Fiber Reinforced Polymer
CNC	Computer Numerical Control
CTE	Coefficient Thermal Expansion
EEPROM	Electrically Erasable Programmable Read-Only Memory
FDM	Fused Deposition Modeling
FDMM	Fused Deposition Of Multi-Material
FDMM	Fused Deposition Of Multi-Material
FGM	Functional Graded Materials
GUI	Graphical User Interface
HIPS	High Impact Polystyrene
LIMDA	Laboratory of Intelligent Manufacturing, Design And Automation
MMAM	Multiple Material Additive Manufacturing
NEMA	National Electrical Manufacturers Association
PA	Polyamide
PC	Polycarbonate
PE	Polyethylene
PLA	Polylactic Acid
PP	Polypropylene
PVA	Polyvinyl Alcohol
SLA	Stereo Lithography
STL	Stereolithography File Format
STL	Standard Tessellation Language
TPU	Thermoplastic Polyurethane
TSE	Twin Screw Extrusion
UAV	Unmanned Aerial Vehicles

Chapter 1

Introduction

This chapter introduces the thesis, describes the completed work, and gives motivation for the research. It also defines the preliminary research questions and highlights the objectives of the research project.

1.1 Background and Motivation

Additive manufacturing (AM), also commonly known as 3D Printing, is a manufacturing technology that is increasing rapidly today. AM begins with a virtual design, which is then printed physically in three dimensions by a printer machine. The AM process works with the principle of a layer-by-layer material deposition process. During the production of a part, the 3D virtual model is sliced in layers to create tool-paths, which is used to manufacture layer by layer until the final part is created.

Notably, in the field of rapid prototyping (RP), additive manufacturing has become indispensable in a wide range of industries, including construction, automotive, oil and gas, aerospace, and medicine. In some applications, additive manufacturing is employed as mass production of end-use parts, i.e., automotive roof mechanisms. Some 3D printers available can be purchased relatively cheap, starting at 700 CAD [1]. Among these 3D printers, fused deposition modelling (FDM) is still one of the most popular material filament extrusion processes in the market. There are some essential factors when implementing the FDM technique. These may include the type and amount of materials a machine can handle, the kind of extruder nozzles, the

printing resolution, the building speed, and others. Most personal 3D printers out in the market, commonly known as fabbers, still produce parts with a single material and without support [2]. A company named Stratasys was pioneered to introduce the first AM system with two dual nozzles. One nozzle is used to extrude the main material to build the part, and the second one is used as a support material [3]. The limitations in FDM systems are mainly in terms of accuracy, build speed, and material. For this last one, an integration of various thermoplastic filaments with significant capabilities on the controller and software to handle multiple extruders, to control the material deposition, and bonding between materials appropriately could solve this limitation. Additionally, most of the 3D printers out in the market are private-source, meaning that it makes it difficult for the user to integrate, modify, or improve the system. For this reason, the complexity of adding new features in a consumer-level 3D printer becomes more challenging to implement.

Although there is notably research in the field of additive manufacturing, and users are actively involved in machine innovation and multi-material optimization, there are areas that need further investigations. The development of a reconfigurable and cost-effective 3D printer with proven application-based research on multi-material products should be explored. The production of parts requires not just the use of traditional manufacturing processes, which were designed to satisfy the needs of products in the past. Currently, the use of AM multi-materials enables the production of extremely complex shape components, enhances the mechanical properties, and can provide new functionality to a part. The research team at the Laboratory of Intelligent Manufacturing, Design, and Automation (LIMDA) developed an experimental setup for AM technology capable of producing multi-material polymer parts with different extrusion modes. The use of multi-material

mixing nozzles enable the production of blended materials by combining different properties to achieve a desired outcome i.e. reinforce critical points in an object where strength and flexibility are required and multiple nozzles extruders can produce multi-material parts to enhance the mechanical properties and provide a more efficient additive process.

1.2 Research Objectives

The research in this thesis focuses on additive manufacturing, its advantages and limitations, and multi-material AM systems, as it is relevant to small industries specifically to manufacturing. The main objective of the research is as follows:

"Develop a cost-effective and reconfigurable multi-material polymer based-extrusion 3D printing process, which can produce multi-material parts via FDM, analyze the influence of linking technology with the mechanical properties, and evaluate the best performance of combining conventional 3D printing materials in an integrated structure".

To develop the thesis framework, the main **objective** is subdivided into the following objectives:

1. Develop a multi-material FDM 3D printing setup that can work with a variety of thermoplastic polymers using either a single-mixing nozzle extruder or multiple nozzles within the same end effector.
2. Compare the capabilities and performance of the multi-material technologies by evaluating the mechanical properties between the fabricated multi-material specimens.

3. Investigate the best material structural arrangement using the sandwich structure concept applied to cost-effective 3D printing materials by evaluating and comparing the mechanical properties with single homogeneous materials.

1.3 Scope and Limitations

This thesis focuses on the development of a multi-material FDM system that integrates and compares two modes of technology: a single mixing nozzle and multi-nozzles extruders. It validates the performance and efficiency of both technologies by printing multi-material samples with different material combinations. It also studies the tensile properties of specimens to compare among conventional 3D printing materials the best material arrangement utilizing the sandwich-structure method. The manufacturing setup developed in this research works within the principle of a Cartesian machine, so its motion is limited to just three axes. The setup is limited to maximum dimensions of the building plate of 200*200*350-mm. It is only able to extrude continuous rigid filaments and can melt materials using either traditional single nozzles, single mixing nozzles (graded materials), or multi-nozzle extruders within the same carriage. As well it can only operate at the most with three materials simultaneously, but it can be upgraded to integrate additional multiple extruders in the future. A new plug-n-play tool head fixture is designed and implemented to enable the use of different 3D printing technologies in the same printer. The maximum heating temperature that the nozzles can reach is 300°C, which indicates that the system is limited to process materials only lower than this melting point. The system works with an open-source firmware so it can be reconfigurable to enable more capabilities such as higher temperatures by switching to a stronger power supplier as well as adding cartridge heaters or any other devices

based on the specific need of the consumer. A general overview of the thesis scope is depicted and described below in Figure 1.1. At the center, the multi-material system is presented, including all the necessary elements to enable and validate multi-material printing. The material selection provides the different types of materials available to fabricate a part. The experimental setup, control and user interface show the components and commands needed for the development of the system. For the fabrication of a multi-material part, it starts from an idea of the specific product, which is then designed, sliced in layers, and deposited on a flat surface. Then, with the use of different types of extrusion modes, the multi-material part can be created and then later evaluate the mechanical properties with an experimental study.

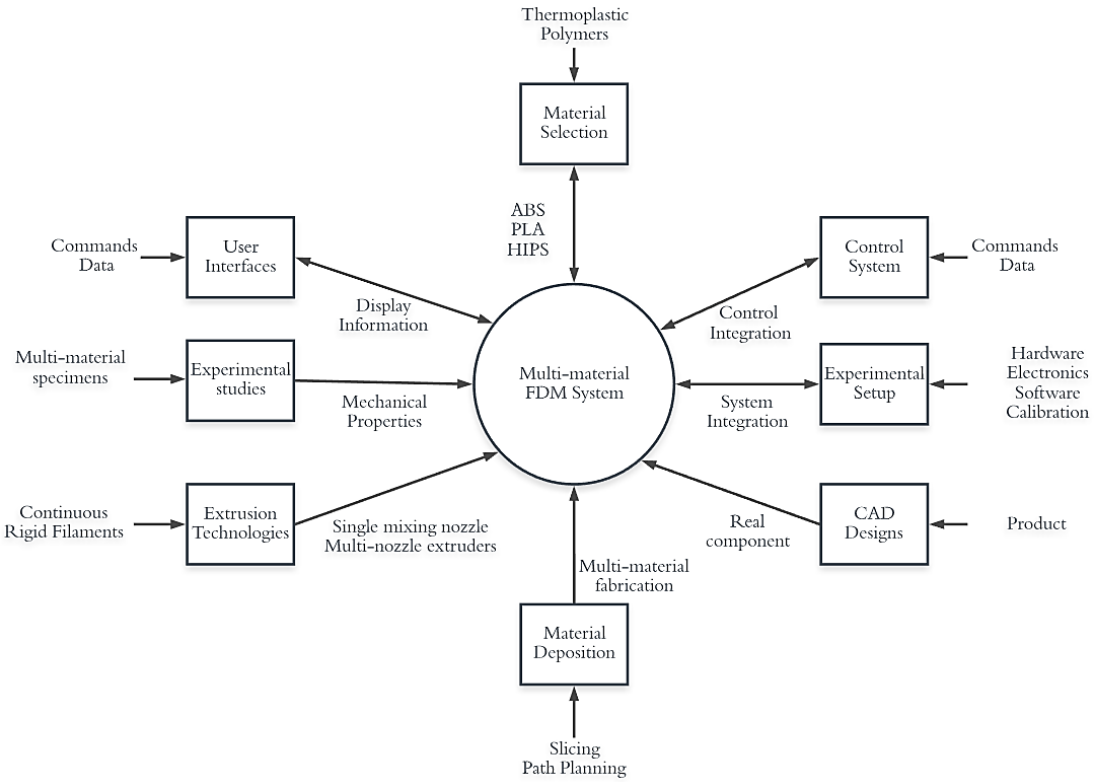

Figure 1.1 Thesis scope

1.4 Thesis Outline

Figure 1.2 shows the thesis layout based on the research objectives, and a description linking the objectives to the chapters is provided below.

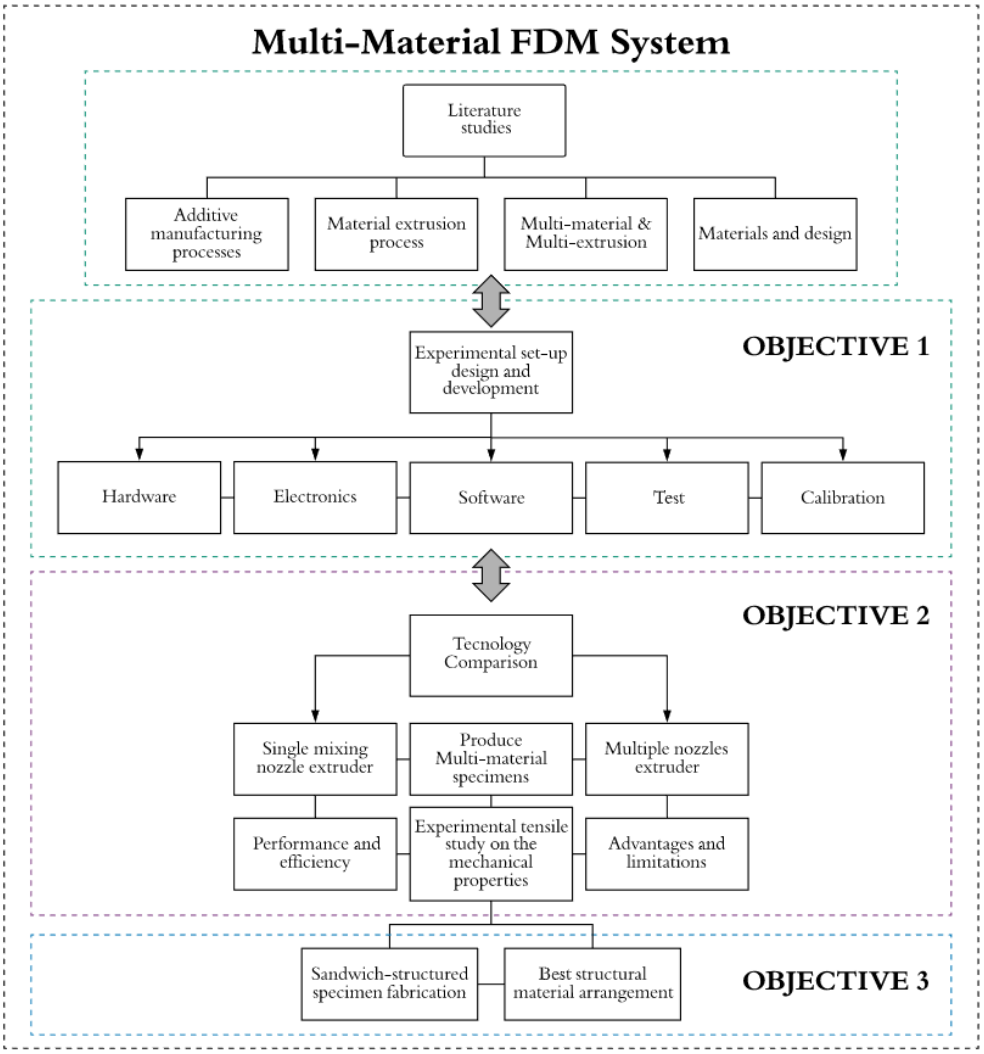

Figure 1.2 Thesis layout according to the research objectives

This thesis comprises six chapters. Chapter 1 present a brief introduction to research motivation, states the research problem, and highlight the research objectives. Chapter 2 presents the literature review of additive manufacturing, fused deposition

modelling, and multi-material 3D printing. Chapter 3 carryout the experimental setup development of a multi-material polymer extrusion 3D printer, including a description of the hardware, software, and system integration by addressing the first research objective. Chapter 4 fulfills the second research objective with validation using experimental tensile test for multi-material specimens through the article "The impact on the mechanical properties of multi-material polymers fabricated with a single mixing nozzle and multi-nozzle systems via fused deposition modelling." Chapter 5 carries out the third research objective by conducting the tensile study to find the best sandwich-structured specimen using conventional 3D printed materials with the article "Tensile mechanical behaviour of multi-polymer sandwich structures via fused deposition modelling." Finally, chapter 6 provides conclusions and summarizes all the research contributions, limitations, and future work directions.

Chapter 2

Literature Review

The presented literature covers the most diverse parts of the research on additive manufacturing, fused deposition modelling, and multi-material 3D printing. Moreover, a description of each type of additive manufacturing process, the most popular AM techniques, and the latest research studies are presented. This literature is required to support the implemented methodologies and solutions to develop a multi-material 3D printing technology.

2.1 Additive Manufacturing

The first concept of additive manufacturing (AM) was introduced in the market in 1987, and by that time, it was well-known as generative manufacturing or rapid prototyping [4]. AM began in the form of stereolithography (SLA), but the mechanical properties of the parts produced were not as higher than the parts made by conventional manufacturing methods [5]. Currently, the general audience and research community refer to AM as 3D printing. In this regard, AM is defined as a process of combining materials to build parts from a 3D model design, usually layer upon layer, as opposed to conventional manufacturing strategies, i.e., subtractive manufacturing [6]. This promising technology is extensively used in science and engineering to produce customized and integrated geometries, prototype models and functional parts.

2.1.1 The Process Chain of Additive Manufacturing

The basis of additive manufacturing begins with a complete CAD volume model of the component to be manufactured. This model is cut off into layers using a slicing software that generates the toolpath planning to fabricate the part. The 3D printer machine is in charge of creating the physical layers on top of each other by gathering the virtual information produced by the slicer software. Ultimately, the machine manufactures the 3D printing part. The process chain is shown schematically in Figure 2.1.

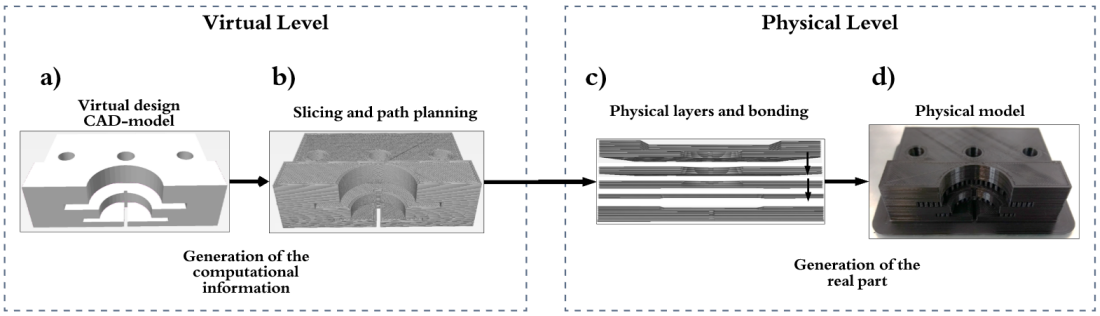

Figure 2.1 The process chain on additive manufacturing; a) CAD-model, b) slicing & path planning, c) physical layers & bonding, d) physical model

A general overview of the AM process is depicted in Figure 2.2. The product represents the part that is intended to be 3D printed. It may be categorized as an idea, an existing virtual part or/and a current physical model. A design using CAD software can embody the product idea. Also, two- dimensional information from an existing object, i.e., CAD drawing, can be converted into a 3D model. The DXF format can be used to convert the 2D projected view to a 3D model. Furthermore, if an existing physical object is to be modified or duplicated, it can be digitized with the use of a coordinate measuring machine (CMM) or digitally captured using a 3D scanner. This latter method is commonly known as reverse engineering, where the

collected data, usually a representation of point clouds from the contour of the model, are transferred into the virtual 3D surface model.

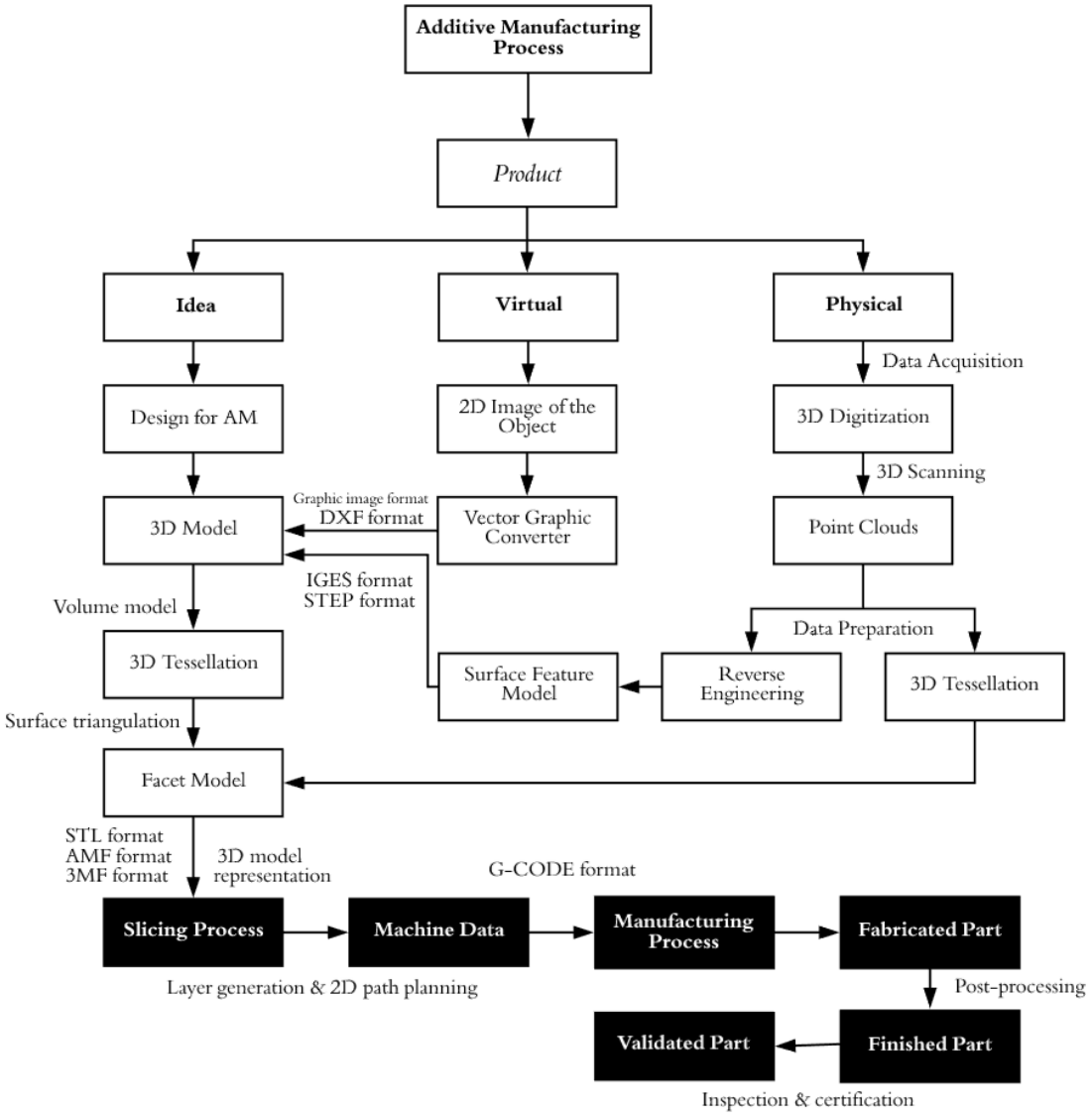

Figure 2.2 A general overview of the decision-making AM process

The virtual design of the component leads to a solid virtual model. The CAD software uses specific file formats to store the CAD information. The STEP or IGES format can be used to transmit or exchange data sets. After producing the volume model, it is required to approximate the model into small contiguous triangles (See

Figure 2.3). This technique is commonly known as tessellation. The exact position and orientation of these triangles are stored in a model format, i.e., STL file data set. To accomplish a more accurate 3D printed model, the triangular surface must be smaller enough to compensate for any volume error.

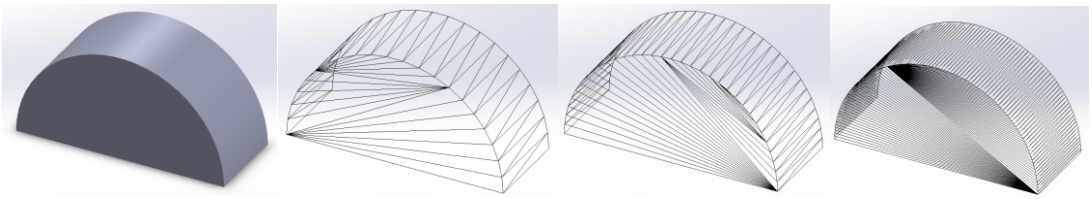

Figure 2.3 Principle of tessellation. A semi-circle model (left) is approximated with triangular facets (right). The more triangles used, the more accurately the model can be approximated

The triangulate faced model is cut into layers by using a slicing software. The x- and y- coordinate information is stored together with the layer thickness. The format used to represent these data set for transfer to the 3D printer is known as G-CODE format. These instructions tell the system how to move geometrically and extrude specified material flow in the different axes. This format follows the NIST RS274NGC [7] interpreter standard, which was developed to read CNC machines. Once the contour data is produced, it is transferred to the 3D printer controller, which builds the physical layers and fabricates the shape of the component. An overview of all the G-code commands for 3D printing can be found in [8].

2.1.2 Classification of AM Processes

There are seven process categories for grouping AM machine technologies that include as follows: binder jetting, directed energy deposition, material jetting, material extrusion, powder bed fusion, sheet lamination, and vat

photopolymerization [6]. The classification of the current processes based on the starting material type is shown schematically in Figure 2.4.

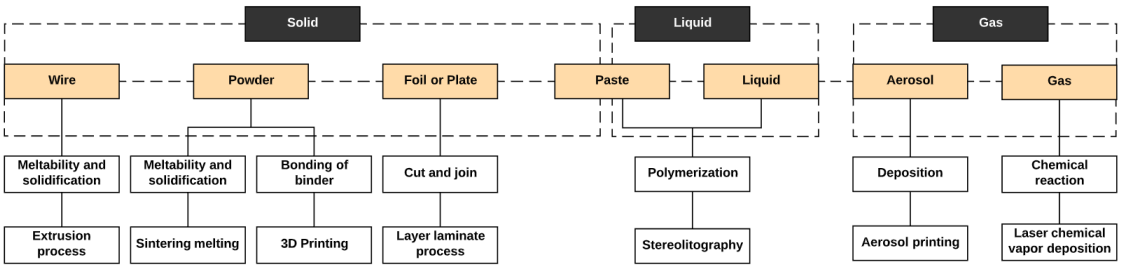

Figure 2.4 Classification of additive manufacturing processes based on the aggregate form of the material according to DIN 8580, based from [2]

In the sintering or melting process, a powder is selectively melted locally using a high-energy laser beam. This heat of source is reflected by the rotating x-y mirror projector and strikes the solidification area. Particles near the solidified zone are combined and gradually form the layer. After a layer is created, the part and the necessary lattice material structure for overhanging features are lowered by the lifting platform. Finally, the sweeper layer fills the powder bed with new powder particles after each consecutive layer. Laser sintering (LS) (See Figure 2.5 left) is one of the best known for this method. Another process that involves powder as a starting material is the binding jetting or known as the 3D printing process (3DP). A binder is applied onto a powder bed that locally bonds the particles together to form the solid layers. After each layer, the part and possible support material for overhanging features are lowered by the lifting platform. Finally, the sweeper layer fills the powder bed with new powder particles after each layer. Figure 2.5 (right) shows the binder jetting process.

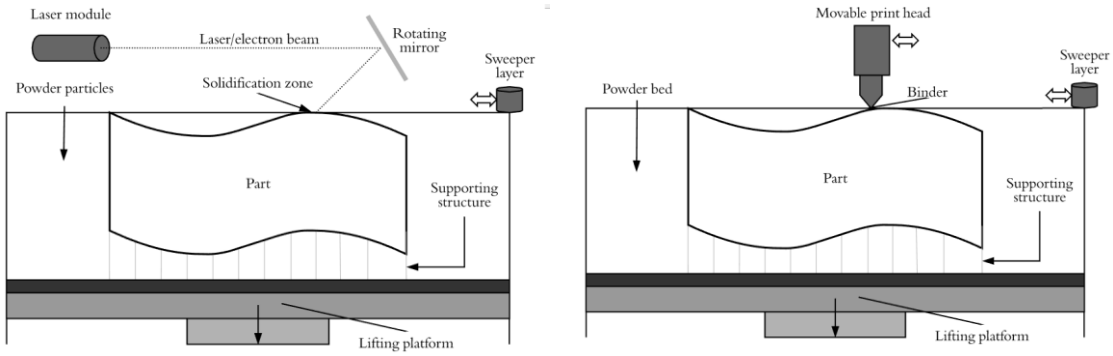

Figure 2.5 The working principle of laser sintering (left) and binder jetting (right)

In the sheet lamination process, the laser beam cuts the contour of the respective layer into the foil strip using the rotating x-y mirror projector. Milling cutters or knives can also be used to contour the layer. Then a lapping roller is used to applied pressure between a layer with the previous one. For the next layer to be created, the part and the necessary support material structure for overhanging features are lowered by one layer thickness by the lifting platform. After a film is employed from the supply roll and the residual film layer is sent to the residual pick-up roll. The method for laminations can be adhesives, plastics, and metals. Layer laminated manufacturing (See Figure 2.6) is one of the best known for this process.

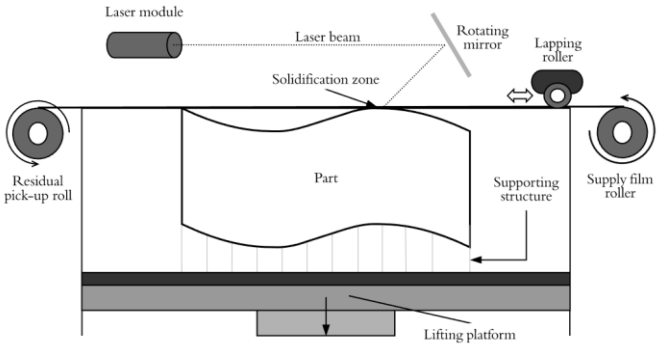

Figure 2.6 The working principle of the sheet lamination process

The wire method consists usually of a thermoplastic filament that is heated up above the melting point. The material is pushed out by an extruder print head and uniformly deposited layer by layer on a surface until it solidifies. This process is known as FDM and is illustrated schematically in Figure 2.7.

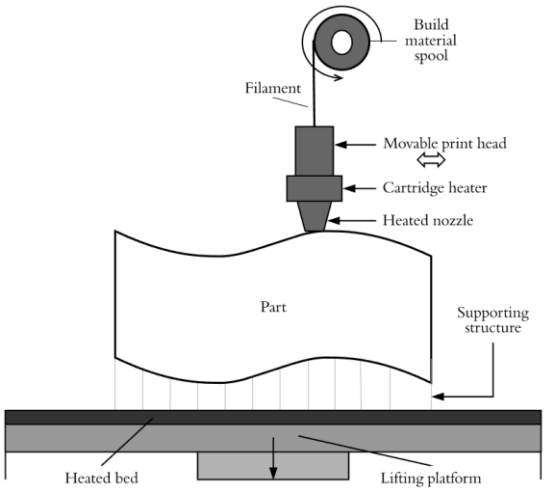

Figure 2.7 The working principle of fused deposition modelling

For the liquids, a vat of monomer, such as an epoxy resin is cured through a locally UV radiation light and thus converts the exposed zones onto the shape of the part layer by layer. The stereolithography apparatus (SLA) is used for this process and is shown in Figure 2.8.

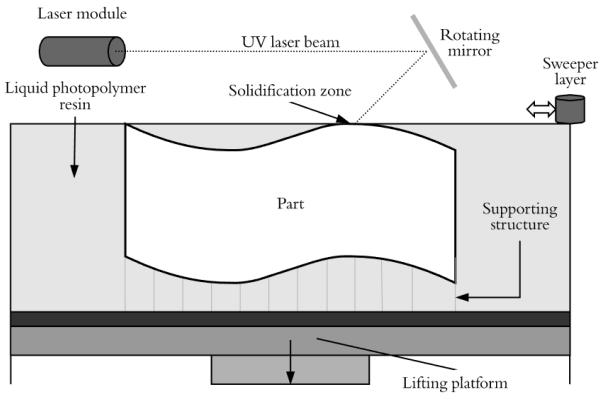

Figure 2.8 The working principle of stereolithography

For the gaseous material, two intersecting laser beams, which are locally positioned, trigger a chemical reaction. Both lasers are sufficiently energetic to start the local reaction. As an example, from a mixture of aluminum and an oxygen-containing gas, solid aluminum oxide can be generated, and structures can be created. The laser chemical deposition (LCVP) is an example of this type of process.

Another example is the aerosol jet printing process (See Figure 2.9), which is used to print substrates with a surface area up to 1µm. A nozzle applies a fine aerosol mixture that transports the material to be printed in the form of particles with a size of 200-nm diameter. After the aerosol is evaporated, heat treatment is necessary to ensure proper bonding to the substrate. This process is mainly used in medicine and microtechnology, where materials such as living cells are fundamental for precise control.

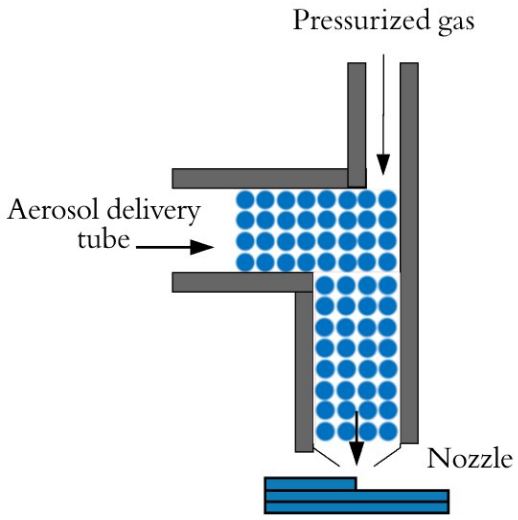

Figure 2.9 Schematic of the aerosol jet printing

2.2 Material Extrusion Process

Extrusion-based processes are the most widely used AM technologies on the market. There are different approaches to be considered for the extrusion, loading, and liquification process of the material. One can classify the material extrusion process in different types of extruders (See Figure 2.10). A plunger-based extrusion is commonly used when the material is in a liquid form. However, most of the material is supplied as a solid in the form of powder, pellet, or as a continuous filament. For the pellets or powders, fed under gravity, typically a screw feeding mechanism is implemented and able to generate sufficient pressure to push the material throughout the nozzle [9]. For a continuous filament extrusion, the well-known fused deposition technique is implemented. The filament is forced to pass through an extruder and pushed into the liquefier chamber and provides an input to generate a precise pressure for the nozzle. FDM is capable of producing a wide range of parts with the use of different materials. After the expiration of some of the FDM patents, the rapid growth of these systems, especially personal 3D printers based on the RepRap open-source project [10], became available. These 3D printers consisted of inexpensive equipment and could be purchased as a complete set and fully- assembled machines.

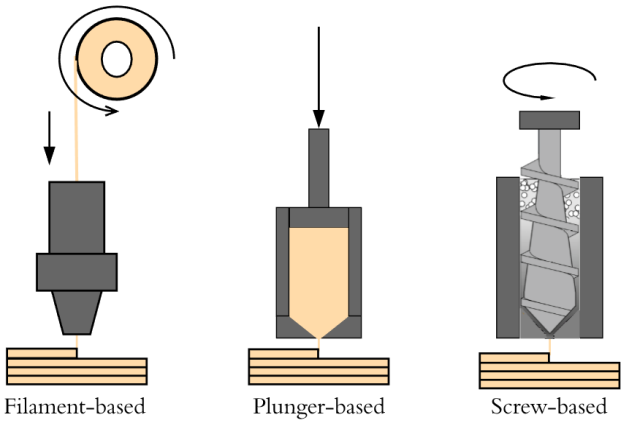

Figure 2.10 Different extrusion principles

2.2.1 The FDM Process

The polymer extrusion FDM process uses an electric heating system to increase the temperature and to melt the material inside the liquefied chamber so it can flow out through the tip of a nozzle and bond with layers of materials before solidifying. The material, usually a thermoplastic polymer, comes out from the nozzle in a semisolid state and hardens with the desired solid shape in the heated plate. It is assumed that the material flows as a Newtonian fluid where the stresses and local strain rate are linearly at every point [11]. If the pressure of the material remains constant while extruding, then a constant flow rate remains. Besides, if the building speed between the nozzle and the build platform is kept constant while printing, then the material cross-sectional diameter remains constant as well [12]. The print head extruder is usually mounted vertically on a coordinated machine. The machine must be capable of starting and stopping the flow rate while creating the contour of the part. It has to precisely enable and disable the motion platforms in all axes automatically while depositing or completing a layer. Figure 2.11 shows the schematic of an extrusion-filament based system.

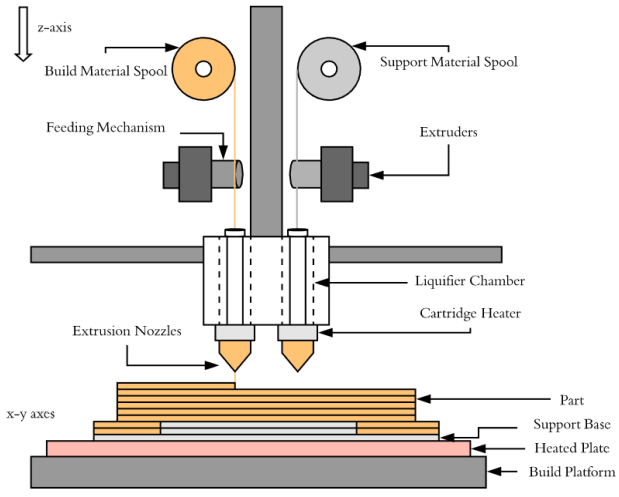

Figure 2.11 Schematic of the material extrusion process

2.2.2 Materials for FDM

The FDM machines available in the market encounter various limitations on the use and type of materials that this technology can handle. The FDM materials can be classified as standard materials, engineering-based materials, and advanced materials [13]. The most common materials for 3D printing and its basic structure are illustrated in Figure 2.12. Thermoplastic polymers are considered the most common and suitable materials for the FDM process due to their diversity, ease of control flow, and a wide range of melting temperatures [14]. However, the building process of AM, which consists of a layer by layer basis, produces parts with anisotropic effects and poor mechanical properties, which are caused by the presence of voids in the deposition path of the extruding material [15]. Anisotropic means that the mechanical properties are different in all directions (cross-section and perpendicular to the part). These properties usually depend on the process parameters of the AM process, such as the infill pattern, orientation, layer thickness, bonding interface, etc. Anisotropy can be reduced by enhancing the extrusion technology with a more suitable heating system inside the machine and deposition of thin layers [16].

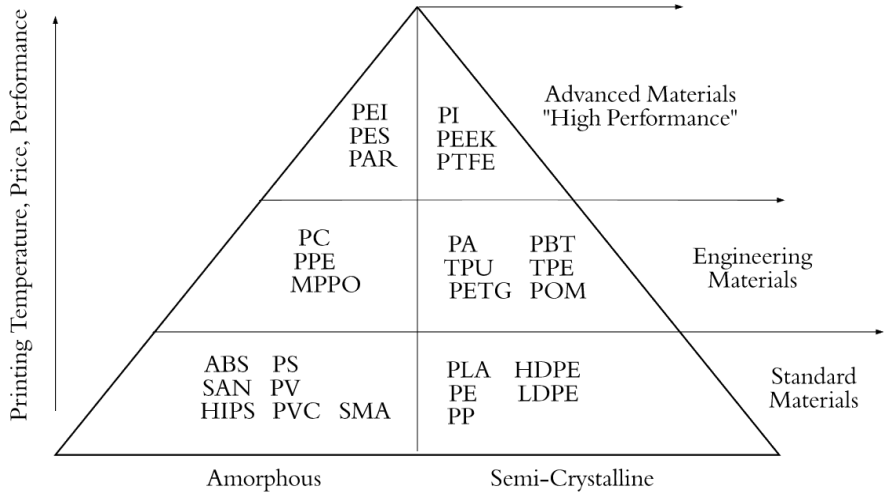

Figure 2.12 Common thermoplastic polymers for 3D printing, based from [16,17]

Research is done to increase the variety of materials and to solve the issue of inferior mechanical properties of 3D printed polymers [18]. Some of the desired features are to increase the strength, stiffness, transparency, and elasticity of a part. Below commonly used thermoplastics for FDM will be briefly discussed, including some of their essential properties to their performance.

The most popular thermoplastic polymers used for FDM are acrylonitrile butadiene polystyrene (ABS) and polylactic acid (PLA) [5]. Other materials can be used based on their chemical and mechanical properties, such as elasticity, memory shape, conductivity, among others. ABS shows good mechanical properties by providing excellent heat resistance and low thermal conductivity. The form of ABS can be represented in different grades and degrees of polymerization, making it compatible with other materials [19,20]. Due to its amorphous structure from the polystyrene property, ABS show high stiffness. Besides, butadiene and acrylonitrile provide toughness and resistance to heat, respectively. The major drawback of ABS in FDM is that it produces toxic gases when it melts, and it can shrink and warp at an early stage while printing because of its internal thermal stresses [21]. To mitigate these issues, an extractor to remove the toxic fumes can be implemented. Also, some other factors, such as the generation of rafts, building support structures, control of the environmental temperature, and heated bed temperature, could help reduce the problem [22].

On the other hand, PLA is well known biodegradable material with a low glass transition temperature, sustainable and with excellent plastic behaviour in the long term [23,24]. Compare to ABS, PLA does not emit toxic fumes, so no ventilation is needed while printing. Nevertheless, PLA formulation usually softens the material around 65 °C, so it may be a problem when it used in a confined heating environment

but also means that it is capable of mitigating internal stresses that may occur when cooling down. Compare to other materials, PLA is mainly used for the production of conceptual parts due to its low impact strength and temperature stability. Another copolymer used in FDM is polyamide (PA), commonly known as nylon, which shows excellent properties such as heat, wear, and fatigue resistance, strong adhesion to the z-axis, provides flexibility in bending, and high strength in tension. However, PA is hygroscopic, which means that it quickly absorbs moisture from the environment, and warping can be presented due to its high coefficient thermal expansion (CTE). This material requires high temperatures to be melted, and some commercial 3D printers are not able to handle such capacity. Another polymer is polycarbonate (PC) which shows high impact resistance, high plasticity, high toughness, and optical clarity, among others. The main drawbacks of PC are similar to the nylon material, in which high temperature is required to melt and extrude the material. High impact polystyrene (HIPS) present high impact strength and low stiffness in tension but provides simplicity for its machinability and production [25]. Ultimately, thermoplastic polyurethane (TPU) is a flexible printable material capable of deforming, elongating and returning to its previous shape when crystalline portions stay intact. It is resistant to degradation and abrasion, which makes it suitable for the production of seals and gaskets. Table 2.1 [26] shows the typical thermal properties of the thermoplastics mentioned above for 3D printing. It also includes the recommended temperatures of the heated bed so the material can adhere properly to the flat surface while printing as well as the coefficient of linear thermal expansion (CLTE) to indicate to what extent the material expands upon heating.

Table 2.1 Typical properties of some FDM thermoplastic polymers, examples

Thermal Properties	**ABS**	**PA**	**PLA**	**PC**	**HIPS**	**TPU**
Melting Temp. (°C)	200 to 240	220 to 270	190 to 240	140 to 230	195 to 240	190 to 220
T_g(°C)	105	110 to 120	56 to 58	140 to 150	100	-25
Bed Temp. (°C)	65 to 100	80 to 100	20 to 50	50 to 70	80 to 95	50 to 60
CLTE [10^{-6}(1/°C)]	86 to 102	124 to 128	85	57 to 72	88 to 90	90 to 170

2.2.3 Multi-material Additive Manufacturing

AM enables the fabrication of products with multi-material capabilities. It allows us to apply a range of materials with different properties selectively and create a new required specification based on the defined application. One can link directly the equipment itself with the performance of the materials for the production of reliable multi-material parts. Multi-materials allow the integration of advanced functionalities, produce more complex geometries, or even replace full assemblies of machined parts. A variety of strategies can be introduced to fabricate multi-material parts. Among these may include the deposition of discrete materials placed to each other, the variation of the material porosity in some segments of a part, or even as a mixture (blending) of the percentage ratio of different materials in a specific zone [27,28]. Some research in combining polymers has been done, including materials such as PLA-PC, PE-PP, ABS-PC [5]; hence, there is an area for improvement on conventional materials for researchers to explore. Similarly, investigations to develop new materials have been considered in recent years, due to technological advancements in fields such as tissue engineering and nanotechnology. Composite materials, which are parts made as a combination of two or more materials, such as ceramic composites, natural fibre reinforced composites, metal and polymer matrix composites are among these new materials that can be used in FDM to optimize the rheological and mechanical behavior into a single material [5]. Also, the use of

functionally graded materials with composites is becoming an alternative to distributing precisely thermal and mechanical stresses in local zones of a part by depositing a graded interface instead of an abrupt change of material that could cause premature failure; thus, makes parts lighter, stronger, and with a low cost [29].

Multi-material systems have been investigated and developed to satisfy the need of customers and product applications. Stereolithography has been one of the widely used processes to assist multi-material printing, but these systems show a time-consuming printing process when changing materials between layers [30]. To enable multi-material in AM, different approaches must be considered to feed and deposit the materials into the system. Some examples of multi-material printing may be found on material jetting technology rather than extrusion-based systems [31]. Multi-material inkjet-based systems have been considered essential for the study of tissue engineering and biopolymer fabrication. Khalil et al. [32] developed a multi-nozzle biopolymer system capable of extruding a controlled amount of cells with a precise position and able to work individually or simultaneously as needed. The system consisted of four different types of pneumatic micro-nozzles, which could work in either extrusion or droplet mode. Some commercial multi-material technologies such as the Object, which uses the Polyjet Matrix Technology, can fabricate parts and assemblies with several materials and control the deposition in specific areas to obtain different mechanical and physical properties [33]. On the metal side, the Optomec LENS system uses a powerful laser with the potential to produce multi-material metal parts by fusing metal powders into a single object.

Regarding the FDM process, usually, dual head extrusion nozzles are found more often in consumer-level 3D printers. The main nozzle builds the part, and the second nozzle makes the support material that works with defined proportions

simultaneously. Besides, a multi extrusion system allows using more than two materials without the need to swap between them manually. Jafari et al. [34] developed a novel multi-material FDM system with advanced ceramics polymer composites and able to deposit up to four different types of materials within a single layer simultaneously for the fabrication of functional parts. Hazrat et al. [35] proposed a multi-nozzle model able to print with five different materials or colours, and the thermoplastic filaments were driven by only two motors using a gear structure mechanism. One of the advantages of having a variety of materials in a single machine is that it enables the opportunity to supply different filaments loaded in the 3D printer and choose the one needed, before starting the print. These varieties of filaments could reduce the cycle time when selecting a specific material. There are no primary technical reasons why 3D printers can not handle multi-materials. Multi-extrusion 3D printing and multi-mixing material extruders are an excellent alternative to produce multi-materials in FDM. These extrusion strategies allow combining different colors of the same material from opaque to translucent materials. They enable to print dissimilar materials for creating hard and soft components into the same part. PVA, for example, is used as a support material for FDM because it can dissolve easily in water after a print, which enables to produce, high-detail and complex integrated geometries. These types of materials provide the end printed part with zero impact on the surface quality and near-zero post-processing effort.

Currently, these promising capabilities of multi extrusion are being attracted by research institutions and companies to solve real issues where the current generation of hardware solutions still come with. However, even some of the common concerns regarding multi-material with multi-extrusion systems may be associated with the alignment of the nozzles, the space needed to accommodate the head extruders, and

dealing with the idle extruders while printing. Besides, how dissimilar materials will interfere with each other to produce an appropriate adhesion is another problem in FDM. Lopes et al. conducted an experimental investigation to evaluate the boundary interface quality and performance of different materials. It was concluded that a proper design on the boundary interface zone must be established at an earlier stage to avoid poor performance in the properties of the material. From the literature studies, it is evident that sufficient research has not been done on linking an FDM system with multi-material capabilities; therefore, a cost-effective multi-material system has been developed to alleviate some of the AM gaps and problems to date.

Chapter 3
Experimental Setup & Development

As mentioned earlier in previous chapters, commercial FDM printers available in the market are mostly private platforms and expensive when it comes to working simultaneously with different materials, which lack flexibility and reconfigurability in terms of the material selection, electronics, control, and software (firmware). These characteristics impede to perform research accurately and free of use. Therefore, the primary motivation to develop a multi-material FDM system would enable research the possibility to integrate essential control devices, to improve the performance of the AM process and to adopt any need and modification as required. In this section, an explanation and analysis of the hardware, electronics, software, and integration of the system are described.

3.1 Hardware Design

A large amount of materials available for the FDM process allows producing a range of multi-materials, which could lead to fabricating parts with an improvement in their mechanical properties. Filament based extruders usually are subject to some performance issues, mainly due to the extruder mechanism. These problems lead to print at low material feed rates, at slow speed and it ends producing geometries with a low resolution. Additionally, when dealing with several types of materials, i.e., PA, PLA, ABS, issues with filament retraction are presented, which is the ability to reverse the filament before depositing a layer of material in the build plate. This factor is crucial, precisely when controlling multiple materials because this prevents oozing during non-extruding movements.

The basis for the experimental setup is customized and assembled from scratch. The system requires to move and handle different multi-material printing heads in the horizontal plane when needed, and capable of holding devices such as sensors, end stops switches, extruders, actuators, power supply, controllers, and any other additional component as required. Thus, considering all these factors, T-slotted aluminum framing was chosen as the main structure of this system. The C shape triple rail used for the linear actuators and the triple profile linear rails with all needed accessories (fittings, corner brackets, spacers, joining plates) were acquired from local and online hardware stores based on the required specifications of the AM process.

The hardware configuration of the system is composed of a motion subsystem and a novel detachable multi-material deposition subsystem. The controllable motion follows the principle of a Cartesian machine with three axes, two in the X-Y horizontal plane, and one Z vertical index plane. The horizontal movements provide the contour and geometry for a given layer, whereas the Z-axis offers the height for each next layer. The travel motion, position, and speed of the three axes require high accuracy and excellent repeatability; therefore, the minimum specifications in terms of load, velocity, acceleration, and printing resolution were established to identify the best components. The motions required to be reconfigurable and allow flexibility for any modifications based on the needs of the multi-material process. The maximum motion capacity for the X-axis was determined based on the weight that it can carry out, which included the different multi-material printing heads, motion plate, sensors, and tool holders. Therefore, high torque trapezoidal lead screws, heavy-duty Delrin wheels, and high precision hybrid stepper motors were selected to ensure high resolution in the system. The mechanical accuracy for the axes motion

was set in a range from 50 to 100 µm and with a minimum standard acceleration set to 750 mm/sec^2. With these considered values, it was determined that hybrid stepper motors with a 1.8° ±5 % step angle accuracy and a holding torque of 12.6 Kg-cm were suitable for the system. Figure 3.2 shows an exploded CAD view of the linear actuator with all its components. An experimental test [36] was conducted to identify the performance of the leadscrew actuators used for this experimental setup. The data showed that these stepper motors have an accuracy of 91 µm, repeatability of ± 39 µm (under no load), a maximum linear force of 115 N and a maximum travelling speed of 8000 mm/min (under no load).

Multi-material FDM 3D printers can be generally broken into two main modes based on the type of extrusion nozzle: a mixing nozzle and multiple-nozzles. Single mixing nozzle multi-material is designed specifically for printing graded materials by mixing a percentage ratio of each type of material in the same geometry simultaneously. Conversely, multiple-nozzle multi-material is designed mostly for the execution of rapid batch production with different contour/raster widths, and different types of materials can be printed in the same geometry as a sequence of different layers generating a combination rather than a mixture of materials. The presented system operates either with single mixing or multiple heated nozzles as a thermoplastic extrusion-based system. The deposition sub-system includes the multi-material hot end nozzles, cartridge heaters, heating nozzles, sensors, a tool holder clamp, and a novel interchangeable plug-n-play rapid tool change adaptor, which are commonly used in CNC machines. The main reason for using a standardized adaptor from CNC is that it will enable future research by combining CNC and AM as all in one hybrid multiple-solution. Also, the advantage of the plug-n-play is that it facilitates the detection of various types of print head components into the system

without the need for physical configuration and provides a setup reduction of the devices and a more time efficiency. The standard mounting tool, a machine taper, is used to grip the tool bit, which is used in CNC for milling or drilling a stock part with high repeatability and with a high-precision. The CAT, BT, HSK are examples of these machine tapers. The deposition of multi-material extrusion was required to be reconfigurable and easily detachable. The minimum requirements in terms of temperature, material, and nozzles were defined to establish the best multi-material extrusion modes. A minimum of three thermoplastic filaments was considered for the deposition sub-system. Then, the highest temperature allowed for the hot-end nozzles to melt a material was set to 300 °C. Ultimately, the printing resolution was set using different nozzles diameters starting from a range of 200 µm to 800 µm accordingly. Different multi-material extrusion nozzles on the market were analyzed, and the diamond hot-end for mixing multiple materials and the Kraken multi-nozzle extrusion were chosen. Figure 3.1 shows the complete model design and assembly of the system, including the subsystem printing deposition for both multi-material modes used for this research.

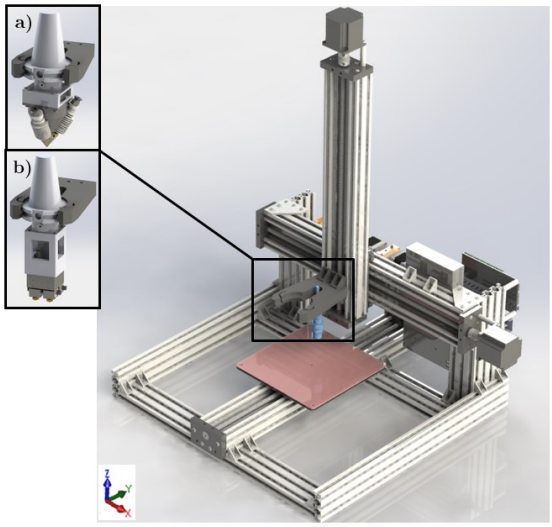

Figure 3.1 Assembly design of the system including the subsystem printing heads deposition a) single mixing extrusion, b) multi-nozzle extrusion

3.2 Electronics and Software

The motion, position, and material deposition of the system was controlled using open-source software and various electronic components. Figure 3.2 shows the control system architecture that was designed and implemented for the development of the system.

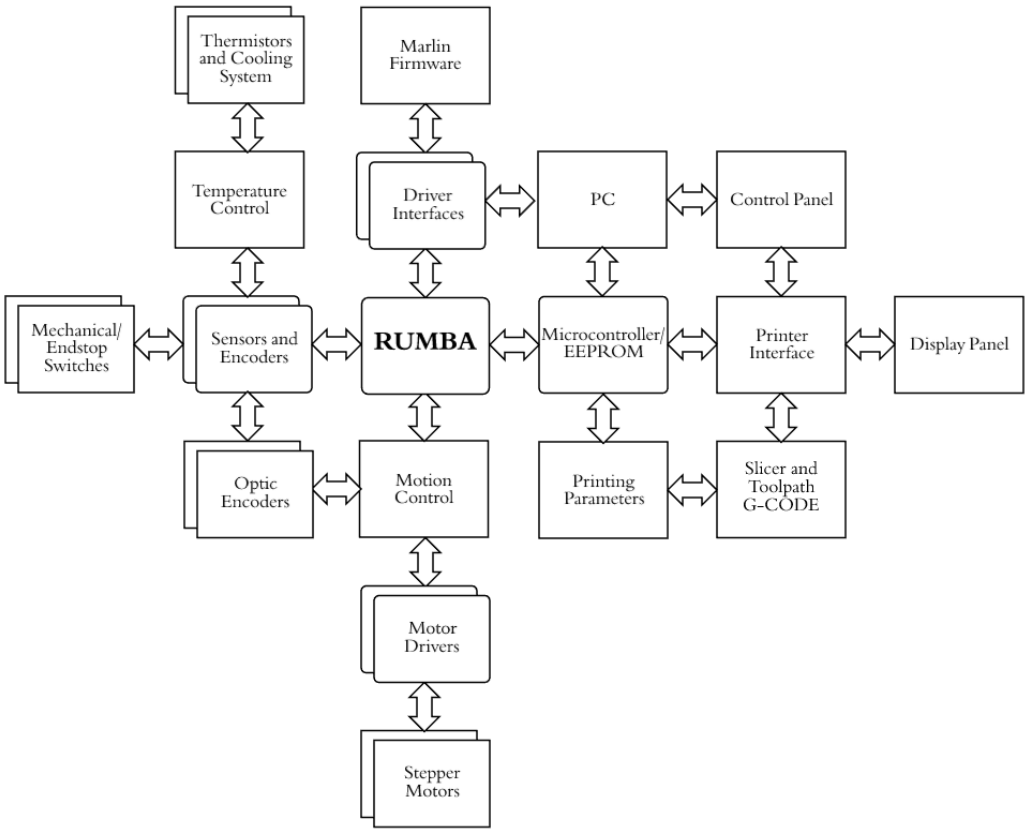

Figure 3.2 Architecture of the multi-material FDM system

At the center level, the RUMBA is the main multi-task controller board that integrates all the necessary inputs and outputs to enable multi-material printing. The board collects and saves the entire machine data, including the printing parameters in the EEPROM integrated into the microprocessor. The memory serves as a buffer, which links the data with the RUMBA, microcontroller, and PC through

driver interfaces and within the main firmware called Marlin. The firmware is executed in an open-source software named Arduino, which provides all the necessary libraries to enable the different parameters to control the system. Also, the RUMBA provides a motion control capacity of up to six motor drivers, three of which are hybrid stepper motors for X-Y-Z axes and three stepper motors used as filament extruders.

To monitor the position of each stepper motor forming the Cartesian configuration, control feedback was implemented from optical encoders attached to the shaft of each actuator. Also, when material runs out from the different filament spools, sensors attached to the extruder motors provide feedback and take actions such as pausing the printing or stopping the whole process. The temperature control can handle up to five independent thermistors, three of which are used to sense the temperature of each liquefier and one thermistor used exclusively for the heated build plate. Additionally, it includes a proximity sensor with a sensing range from 3-mm to 12-mm for auto-leveling the heated nozzle from the flat building surface. A single control panel can execute the system and displayed the data on the screen, just like the consumer-level open-source 3D printers available in the market, i.e. RepRap-based 3D printers or can be commanded directly with the use of a PC using alternative open-source interfaces. The software implemented in this system has to satisfy the needs of multi-materials; therefore, two software interfaces approach for 3D printing were implemented. The first approach was the use of an existing commercial platform named Repetier to 3D print multi-materials, and the second approach was the development of a new graphic user interface to control in real-time the multi-material deposition. Figure 3.3 compares the process architecture between

conventional single-material and the one used in this thesis with multi-material FDM additive manufacturing.

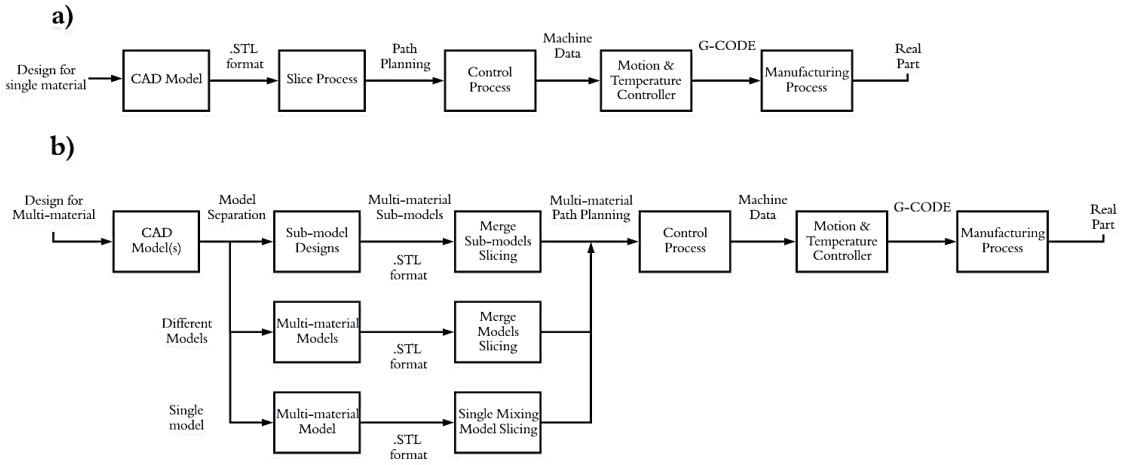

Figure 3.3 Process system architecture between a) single material fabrication b) multi-material fabrications

The process of a single material deposition starts by creating the CAD model, and it is saved in a 3D printing file format, i.e., STL format (.stl). The STL format is the most common method to represent the 3D model information and process of the slicing layer basis in additive manufacturing [37]. This file is then imported in a slicer software which position/orients the part on the actual coordinate system envelope and creates the 2D path planning/ toolpath. After that, support structures are added if necessary, and machine data in a G-CODE format is generated and executed for the fabrication of the part. On the other side, the multi-material process works within the same principle, except that it has different approaches to fabricate a multi-material part. The first one requires splitting the part into single sub-models designs for each specific material, which is then saved individually in an STL file format. Commercial software such as Builder 3D, Autodesk Netfabb and Meshmixer can be used to separate the CAD model. The second approach happens when different CAD models are needed to be fabricated using different materials but in

the same printing process to create multiple part, i.e. batch of different parts. The third one is implemented for the fabrication of graded materials with a mixing ratio in a single part. For the three multi-material methods, a commercial software, Repetier user interface software, provided the capacity to handle multi- material processes and was used to generate single unified models from the different sub-models. Besides, a graphical user interface (GUI), which is still in early stages, was developed and used primarily to test the deposition of different materials in a sequence of contour layers, but it is limited to only single models (See Figure 3.4). For the multi-material slicing process, commercial software are available such as Slic3r, Skeinforge, CuraEngine, and others. Similarly, the developed interface integrates itself with the slicing contour process in its programming. Finally, the tool path planning is generated for each sub-model including the type of material and the submodels are merged into an individual complete final model. Figure 3.5 shows the Repetier platform used for the experimental studies with some multiple material parts as an example.

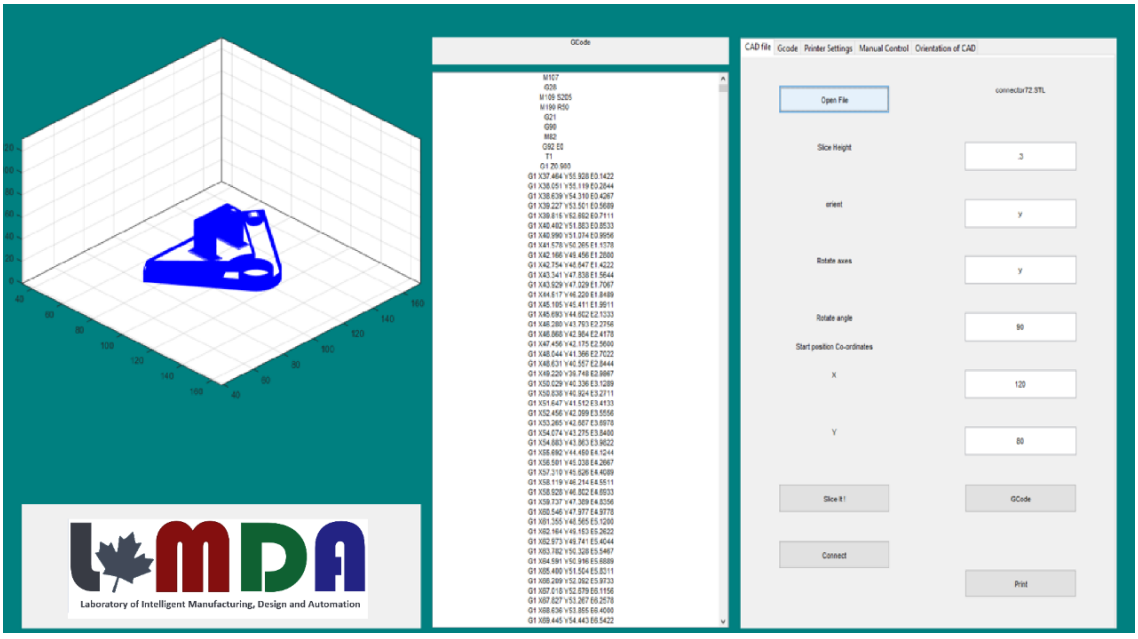

Figure 3.4 LIMDA graphic user interface (GUI), conversion file and process screen

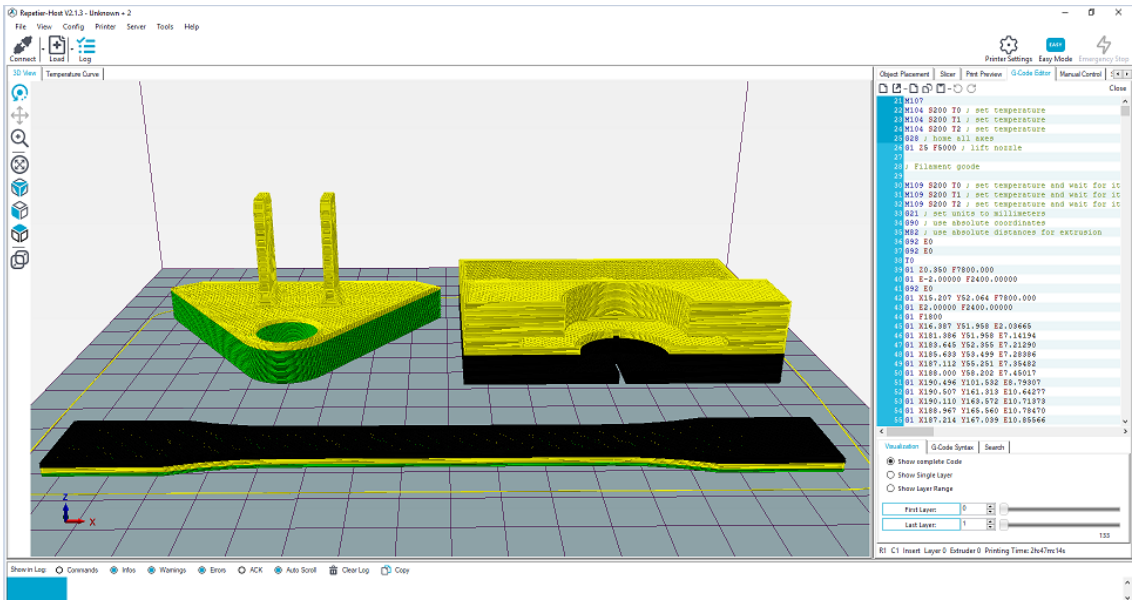

Figure 3.5 Commercial Interface with multi-material parts, examples

In order to execute the system using the developed interface, several steps were involved in generating and integrating an all-in-one solution software architecture (See Figure 3.6). A brief description of what is contained in each subsection is presented below. The CAD model design is saved as an ASCII STL file format to make simple the reading and the manual inspection of each vertex and orientation of the facets. This file is imported in the slicing process with a predefined part orientation, which could be modified to a suitable printing position. After having the part oriented, the slicer finds different possibilities to intersect the triangular facets with the cutting Z plane, which is set by the specific slice thickness. Then, the slicing algorithm connects the segments into a closed contour geometry for each slice at a time. The path planning using optimization algorithms generates the sequence, which is then translated into the G-CODE format. It contains all the printing parameters and commands required to perform the execution of the printing part. These parameters are readable through the GUI and sent via serial communication

to the controller. Finally, manual testing commands are employed and the process information is sent to the machine for the fabrication of the part.

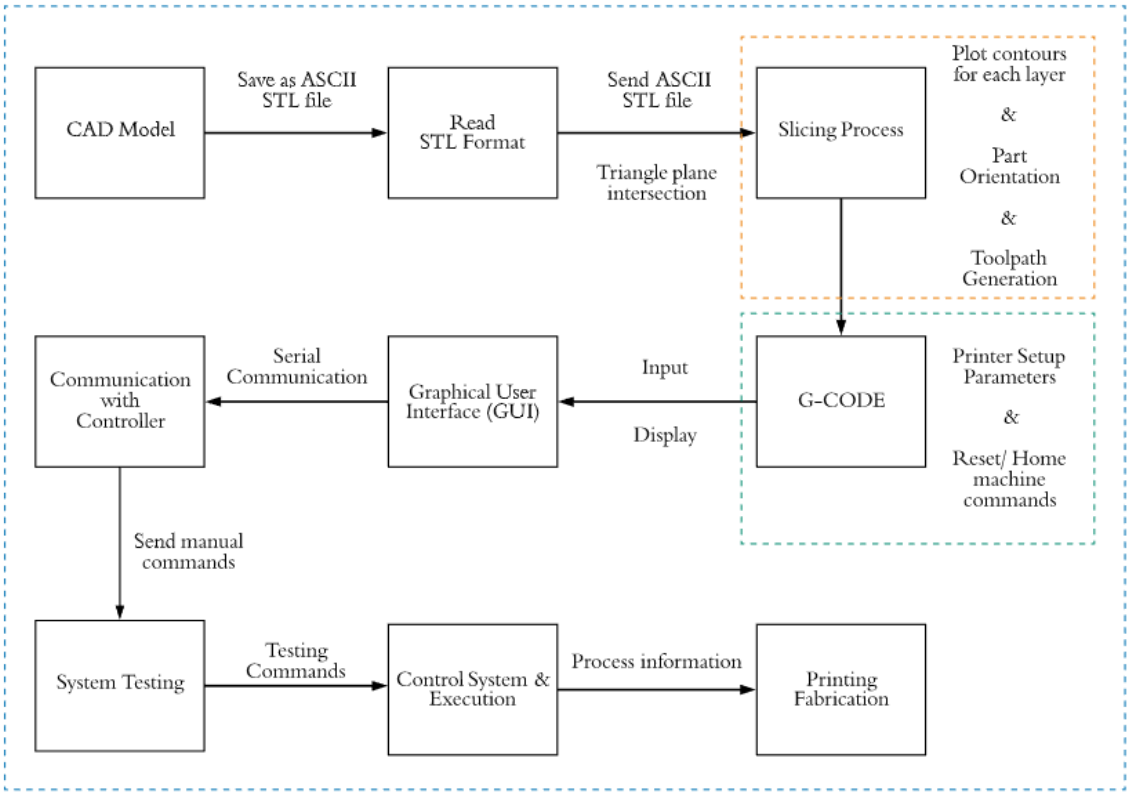

Figure 3.6 LIMDA software architecture

3.3 System Integration, Testing & Calibration

The system integration starts by collecting all the material described in previous sections of this chapter. To build an accurate system, all the mechanical components are assembly under the designs and simulations created early. The support structure, the aluminum framing, is arranged in several long and short rails to provide strategic mechanical support. The use of cast corner brackets, spacers, and bolts put together the linear rails. Also, each stepper motor is attached in its respective axis frame (X-Y-Z axis), and the extruder stepper motors, which are in charged of pushing the

filament to the heating nozzle, are positioned strategically in the back of the system with special design holding brackets. The leadscrews, motion plates, ball bearings, and others are also part of mechanical integration.

With the system frame assembled, the next step is to install all the electronics. Following the datasheets and the electronic circuits of the central controller, as well as most of the components such as power supply, sensors, encoders, motors, coolant pumps, drivers, heating cartridges, and others, the connections and electric wiring, are implemented. After reading the electrical drawing and identifying and installing the electronic devices, it is time to power on the system and make sure it is running correctly to begin with the testing and software configuration of all the components. In order to calibrate the system to get an optimal printing resolution, a micro-stepping configuration for each stepper motor was established. To obtain these values accurately, the use of a multimeter was needed to measure the reference voltage of each motor driver and adjust it accordingly to provide sufficient current for the stepper motors to work efficiently without overheating.

In addition, an auto-levelling sensor is attached to the extrusion deposition subsystem to reduce possible errors while printing. Also, it was necessary to find the offset values of multi-extruder nozzles to provide the best bonding interlayer between materials. For the printing calibration, several parts were tested using some online calibration sets [38,39]. Figure 3.7 shows a rear view of the system with the electronics and electrical wiring connected to the mainboard. In the next chapters, the validation of the system printing with single mixing nozzles and multi nozzles for multi-material parts is presented. Along with its performance, capabilities, and drawbacks of both modes. Ultimately, the mechanical properties of different material

combinations are presented to find the best optimal multi-material arrangement among conventional FDM materials.

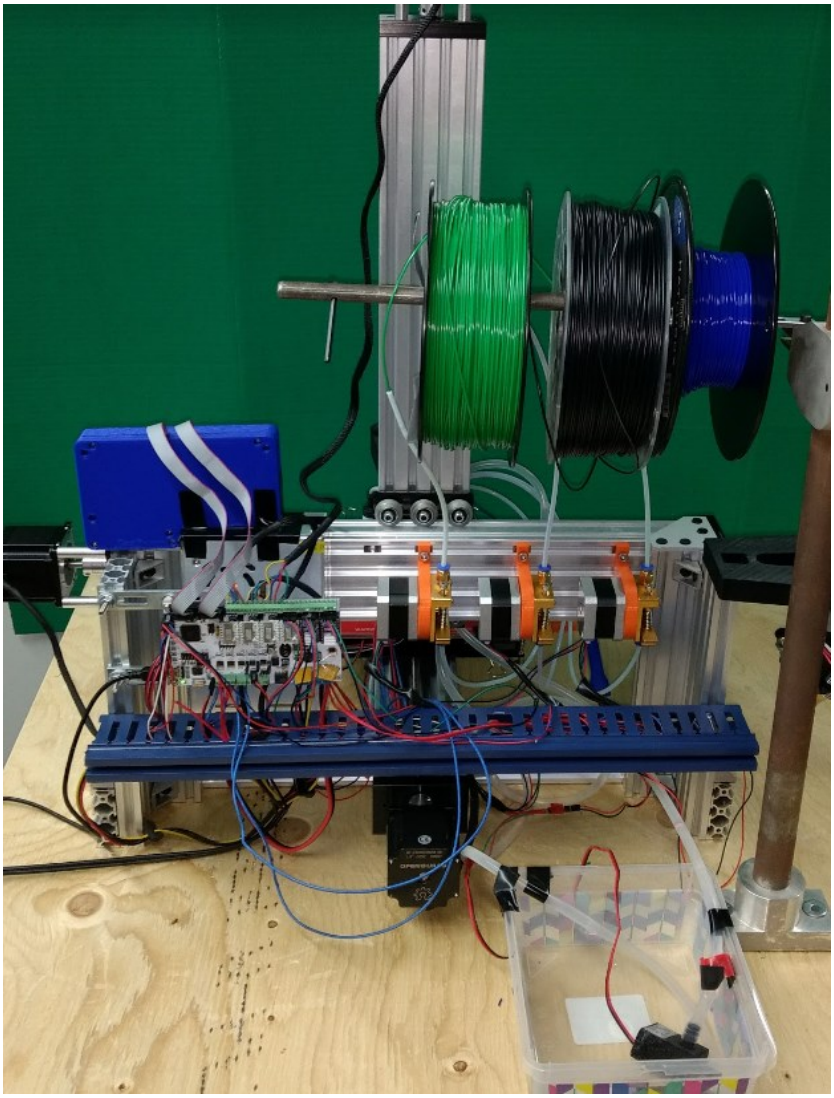

Figure 3.7 Rear view of the electronics and electric wiring of the system

Chapter 4

The impact on the mechanical properties of multi-material polymers fabricated with a single mixing nozzle and multi-nozzle systems via fused deposition modelling

4.1 Introduction

Additive manufacturing (AM) describes a process of combining materials with building parts from a 3D model design, usually layer upon layer, as opposed to conventional manufacturing strategies [6]. To date, this promising technology has gained popularity in developing multi-functional parts with a wide range of complexities that would not be possible using traditional manufacturing processes.

Among these 3D printing processes, fused deposition modeling is the second most popular material extrusion technique in the market [40]. The FDM process consists of a thermoplastic filament, which is extruded through a heated nozzle and uniformly deposited layer by layer on a flat surface [41,42]. Consequently, sliced layers are created and converted into G-code using pre-processing software packages [43]. This AM process has enabled new ways to produce parts more efficiently and solve unique application problems. Previously, the FDM process was limited to a short range of materials, including PLA, polylactic acid, and ABS, acrylonitrile butadiene styrene. These materials satisfy the needs based on their printing easiness and mechanical properties, respectively [44]. PLA shows advantages against other polymers because when degradation occurs, no contamination is released to the environment. Secondly, it shows excellent biocompatibility, so it is widely used for medical purposes, i.e.

tissue engineering. Thirdly, it has remarkable plasticity and toughness in long-term use [23]. ABS for extrusion printing presents heat resistance, high impact resistance, and toughness, which can be increased by a proportion of polybutadiene to acrylonitrile and styrene [45]. High impact polystyrene (HIPS) provides the simplicity of fabrication and low-cost impact strength [46]. Presently, various types of non-conventional materials help produce advanced strength parts and enhance desired properties [5]. It allows 3D printing multi-material parts in a wide variety of forms and in a way that different materials can be deposited in various sections of a region [47] or as a mixture of different materials varying the percentage ratio in the same section, i.e. graded materials and blended composites. Thus, producing multi-material using conventional and non-conventional materials may improve the mechanical properties of a part, add multi-functionality and enhance the performance of the AM process [27]. Since FDM is a low-cost technique, it has the potential to fabricate multi-material components and be applied in the area of mechanical and civil engineering, especially in structural applications [46].

Despite the importance of multi-material in the FDM process, no major work can be found in the literature regarding linking technology to mechanical properties that are used to produce multi-material parts, mainly focusing on the relationship between the equipment itself (single mixing nozzle and multiple- extrusion nozzle) and the mechanical properties of the printed part. The selection of an appropriate multi-material nozzle technology is still a significant challenge because it requires a deep understanding of the control parameters, software capabilities, and electronic components in the 3D printer machine to fabricate an adequate multi-material product.

The primary motivation of this paper is to investigate the effect on the mechanical properties of combining different sections of a part using conventional 3D printing materials (ABS, PLA, and HIPS). Based on the technology used to print multi-material parts from multiple filaments, it exploits a comparison of the technology itself of a single mixing nozzle and multiple nozzles within the same carriage. For strength to materials combination, the comparison addresses an overview of benefits and drawbacks between both extrusion modes, mainly on their capabilities as well as the performance of specimens by conducting experimental tensile testing. Therefore, the contribution of this paper lies in the comparison of the two modes of technology to select the best manufacturing process based on final product performance. Experimental evaluation and demonstration of the mechanical properties of the materials are implemented, and the best process selection of the optimal mode to 3D print a multi-material part is presented. Additionally, efficiency in terms of build time and setup time is explored. The collected data and recommendations will help the user choose a suitable model for future printing requirements using multi-materials for FDM.

4.2 Literature Review

The advantages of the FDM technique can be described as inexpensive to operate from the user perspective as well as the ability to arrange multiple filaments from the fabrication perspective [48]. As FDM technology grows, new methods of printing multiple materials are evolving The study of discrete materials placed next to each other when generating supports, binders used to infiltrate porosity in some segments of a resulting part and blending different materials to fabricate functionally graded components are among these approaches [27]. Furthermore, multi-materials are being

used to reinforce critical parts to increase strength and improve flexibility by finding optimal adhesion between different thermoplastics [49]. Now, focusing on the limitations and some of the actual challenges encountered with the potential of multi-material 3D printing can be classified in the level of the equipment, the part design, and printing materials [47]. For the hardware itself, the number of thermoplastic filament inputs and the ability to combine multi-material restricts existing FDM machines. A few tools like the Bowden extrusion concept for multi-nozzle extrusion systems [35] are capable of feeding rigid filaments away from the printer's heated nozzle but not compatible with flexible materials. Another challenge in the equipment level is maintaining a precise alignment between the nozzles and the heated bed. It requires the user skills to manually calibrate the nozzles or use auto-nozzle leveling when switching the active extrusion head. In regards to the part design and type of materials, a boundary interface is always formed based on the discontinuity of different sections of different materials that have a severe effect on the mechanical behavior of the printed part. Some critical factors that can affect the mechanical properties while printing includes the infill speed, infill pattern, material type, and material content; as well as the extruder temperature and bed temperature, among others. Therefore, the process parameters of FDM show an extremely interrelationship between the characteristics of an end-of-life product [5].

A considerable amount of research papers in the multi-material sector contribute well to the design of systems capable of 3D print multi-material parts to optimize the mechanical properties and to improve interfacial bonding between materials. For the filament extrusion-based systems that support the deposition of different materials, the MK3 FDM 3D printer [50] provides a rotating pulley mechanism to switch up to five different materials using a single-nozzle and includes a new direct-

drive mechanism. This mode is suitable to print different materials in a single part but not able to do mixing materials mainly due to its mechanical design, i.e. switching between filaments one at a time.

A novel approach [51] to FDM multi-material 3D printing was used by combining two dual nozzle FDM printers into a single system incorporating a pneumatic slide in-between them. A sophisticated and robust system was needed to integrate multiple systems to function with each other. Another novel approach [35] proposed a multi-nozzle model using five different multi-color and multi-materials working simultaneously and without halting the process of switching between filaments. On the other hand, a novel investigation [52] of bonding between two different materials in a multi-material print was performed to predict the best parameters to maximize print strength. The 3D printing setup used on this previous investigation was a standard dual nozzle, and the experiment was conducted with only two types of polymers, ABS and TPU. These proposed systems show evidence on the work carried out for the implementation of multi-material extrusion 3D printing. However, which nozzle extrusion model is suitable to print a multi-material part, has not been yet explored in detail.

Additionally, the main issues encountered with fabricating a part using the respective technologies are not well justified. In the literature, these machines either use a multi-nozzle, multi-material technology, or a single nozzle, multi-material in a single machine. A few 3D printer multi-material machines are available on the market, but in the case of combining several materials, the performance and capabilities reduced significantly, especially for the FDM process.

The lack of specific information regarding multi-material extrusion nozzles and the influence of multi-materials based on experimental tensile tests was the primary

motivation of this paper. A comparison of two different technologies within the same machine setup is presented. A decision making- matrix was generated to display their performance in conformity with the ASTM D638- Type 1 specimen for the tensile test [53]. It fosters a better understanding of the behavior of multi-materials printed within the same component with different modes and choosing between part design and technology selection.

4.3 Experimental technology: multi-material extrusion nozzles

The performance of an extruder nozzle in FDM 3D printing enables the capabilities to build multi-material parts, to enhance new products and improve the mechanical properties of a specific component. The concept of fused deposition of multi-material (FDMM) [54] can be classified into two main subgroups, as shown in Figure 4.1: Multi-material single mixing nozzle and multi-material multiple nozzles. In this work, we are considering the E3D Kraken multi-nozzle [55] and the diamond hot end single nozzle [56] models that support multi-material 3D printing.

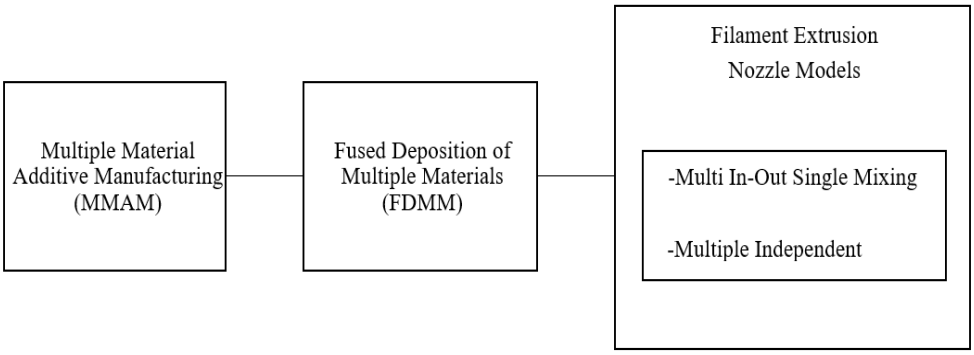

Figure 4.1 Classification of FDM multi-material hot end nozzles

4.3.1 Multiple mixing single extrusion

A multi-in-one-out single nozzle allows you to extrude multiple colors and materials with the same nozzle and can obtain mixed filaments and produce gradient materials [48]. Either the single mixing nozzle uses the same working temperature to melt multiple input filaments or within a range of temperatures between different polymers. Otherwise, it will generate a contaminated final product. For this reason, materials need to have a close relationship in their melting point to obtain effective bonding and quality in different parts of a print. The author [50] suggests that small temperature changes between filaments can be done during printing the purge tower or using the wiping into the infill. This approach reduces the material transition after each filament change.

The advantages of using a single mixing nozzle are that for each layer base, there are no calibration defects when depositing material [48]. In this work, the diamond hot end nozzle was implemented (See Figure 4.2). For this model, the printing sequence was only performed in sections within the same specimen and with different materials. The materials implemented were ABS, PLA, and HIPS. Although this model can do material mixing, for this comparison and evaluation, it was used as a one-by-one material deposition.

Figure 4.2 Mixing nozzle hotend (three inputs and one output)

4.3.2 Multiple extrusion nozzle

Extrusion-based AM systems typically use two or more separate nozzles mounted side-by-side on the same carriage to build multi-color and multi-material components [35,57]. The use of multiple nozzles can facilitate the production of several printing parts by increasing the processing speed by a continuous operation [35]. One of the main challenges using multiple nozzle arrangement comes with the calibration and oozing issues due to idle extruders [48]. This last issue is generated when the next nozzle to be used is heated up and reaches the melting temperature of the polymer, causing drops of material while printing. It requires disabling one of the hot end nozzles while the other is printing. The authors [57] investigated this issue and suggested a toolpath planner for optimizing the part orientation and travel motions to reduce or hide defects. Another approach towards mitigating this issue is to enable the filament retraction for each polymer before it prints in addition to printing the purge tower when switching to another material to print a section.

The advantages of using several nozzles allow placing nozzles of different diameters in the same carriage. These different sizes enable the models to be printed quickly or with fine details, to replace clogged nozzles easily or even build different thickness layers of materials depending on a specific application. These benefits can improve the resolution, functional, and mechanical properties within the same part. In this work, the Kraken hot end multi-nozzle was implemented (See Figure 4.3).

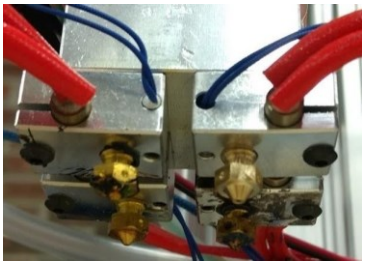

Figure 4.3 Multi-nozzle extrusion (four independent nozzles)

4.4 Experimental Strategy

4.4.1 Equipment and materials

The 3D printer used in this investigation was customized and assembled with structural aluminum frames commonly found on desktop CNC machines. Additionally, it integrated 3D printing components, including the heated bed, nozzle extruders, sensors, mechanical components, and electronics. The control electronics included the Arduino Mega 2560, stepper motor drivers DRV-8825, stepper motors NEMA 23 for the axis travel motions, and stepper motors NEMA 17 for the filament extruders.

The heated bed was calibrated using the Mitutoyo dial indicator with an accuracy of ± 5 µm, and a capacitive sensor was mounted in the Z-axis to auto-level the heated bed with an accuracy of ±10 µm.

The 3D printer is capable of handling both models in the same machine. Nozzle reconfigurability with a manual, standardized, and detachable system was implemented. The two types of multi-material hot end nozzles used were: a multi-in-one out 0.4 mm single-mixing brass nozzle diameter and four separate hot end brass nozzles on the same carriage with a 0.4 mm diameters each. For this last model, it was required to find the offset values between each nozzle to ensure that once it starts printing, an overlap between layers exists. A 0.3 mm heated glass plate was placed on top of the heated bed and used as a printing bed. Figure 4.4 illustrates a general description of the components for both modes implemented.

The two modes mentioned above were used to fabricate the specimen tensile test D638- Type 1 [53] with a 1.75 mm diameter using various material filaments, including PLA, ABS, and HIPS. The filaments were acquired through commercial

suppliers. The following two scenarios and material combinations were considered to evaluate the mechanical performance of the specimens as well as the efficiency of both models:

- Multi in-out single mixing nozzle:

  ABS-HIPS; ABS-PLA; PLA-HIPS; ABS-HIPS-PLA
- Multiple hot end nozzles:

  ABS-HIPS; ABS-PLA; PLA-HIPS; ABS-HIPS-PLA

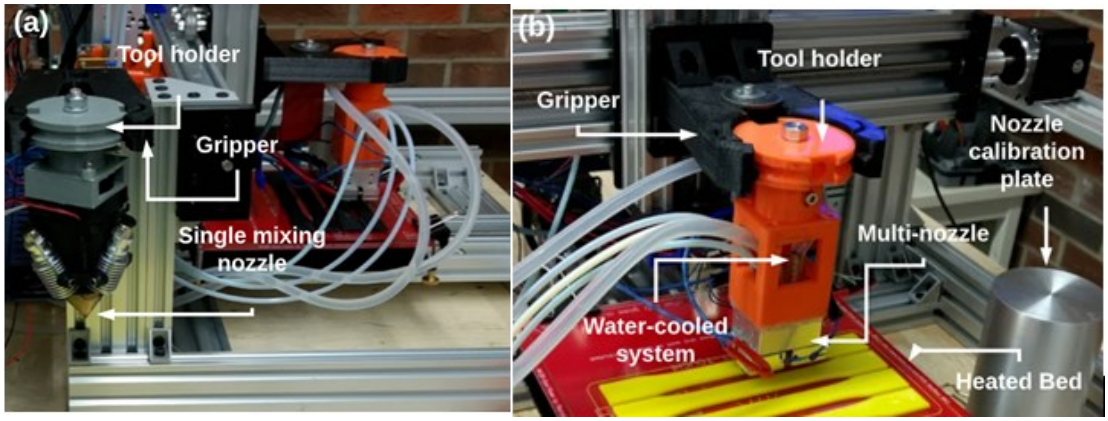

Figure 4.4 Setup developed at LIMDA for a) single mixing nozzle and b) multiple nozzles for the multi-material FDM system

The marlin firmware open-source, Slic3r G code generator, and Repetier interface were used to interact and control the 3D printer to build the specific specimen part. The geometry of the specimen was exported as an STL file using the SolidWorks software. The main dimensions of the specimen are shown in Figure 4.5 [53].

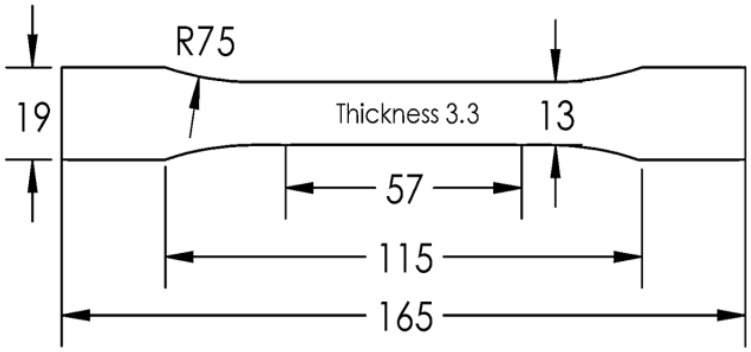

Figure 4.5 Standard specimen for tensile test, dimensions are in mm

4.4.2 Methodology and process parameters

The experimental tensile test was conducted to collect data from the mechanical performance of each multi-material specimen. According to the standard, each specimen was printed five times with each model for the comparison. A total of 70 specimens were printed and tested. It was expected that the methodology would show which nozzle extrusion model is suitable and display the best performance considering fixed and the same parameters for both models to validate their comparison.

To select an appropriate nozzle model, two strategies were implemented:

(1) Multi-material section specimens printed with one, two, and three materials using a multi in-out single mixing nozzle.

(2) Multi-material section specimens printed with one, two, and three materials with a multiple- hot end nozzle.

The experiments considered constant printing parameters for the multi-material 3D printing process. A description of these values are shown in Table 4.1 These parameters were configurable based on the Slic3r Software for single multiple mixing and multiple extruders.

The test specimen was printed with an infill speed of 25 mm/s. The layer thickness was set as constant to 0.3 mm. The recommendation to select the right layer thickness indicates that it should not be greater than 80% of the nozzle diameter [58]. For these experiments, 0.4 mm nozzles were implemented and thus adequate to the layer specifications previously described. A single orientation in the horizontal plane was used for all printed specimens, where the fibers and bonding are better than in other planes[59]. The infill pattern implemented was rectilinear with an infill angle of 45°.

Table 4.1 Constant parameters for 3D printing

Parameters	**Values**
Infill Pattern	Rectilinear
Infill Speed (mm/s)	25
Travel Speed (mm/s)	100
Retraction Speed (mm/s)	5
Infill Density (%)	100
Flow rate, %	100
Infill Angle	45°
Layer Height (mm)	0.3
No. of Shells Perimeters	3
Material Content (%)	33.3, 50
Bed Temperature, °C	90
Nozzle Temperature, °C	240

Consequently, the specimen was printed as a complete body with a different material combination using both modes. Based on the total specimen thickness of 3.3 mm, the material content was assigned as two and three material sections. For the bi-material combination of a specimen, six layers of material were considered at the bottom and five layers at the top. On the other hand, for the tri-material combination, fourth layers of material were considered in the bottom, three layers in the middle, and four layers in the top. Eleven (11) layers of filament were printed

per specimen. Figure 4.6 shows a list of the different material combinations of ABS, PLA, and HIPS used to validate the comparison of both models.

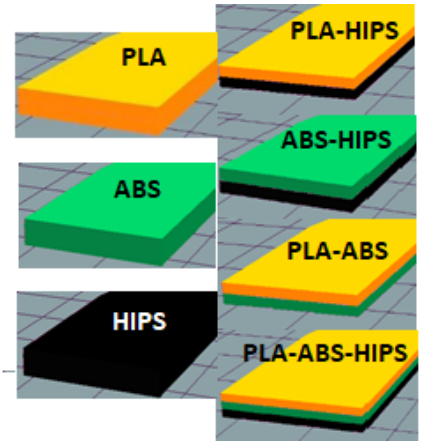

Figure 4.6 Simulation of specimens fabricated with a single material and multi-material

The tensile tests were performed using the Instron 5966 test machine with a minimum speed of 2 mm/min, a load cell of 10 Kn, and a gripper with a maximum load of 5 Kn. Figure 4.7 shows a specimen being tested in the tensile machine. The specimens were loaded along the longitudinal axis until failure was encountered.

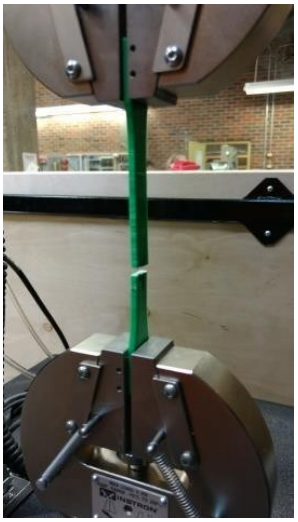

Figure 4.7 Specimen ABS positioned and tested in the tensile machine

4.5 Results and Discussion

This section discusses five main features which address and validate the performance of each mode based on the mechanical properties shown on the specimens tested:

- Tensile strength
- Young's modulus
- Tensile elongation at break
- Build time
- Set up time - Calibration

The results obtained from the tensile test indicate minor differences between the specimen printed with the single mixing nozzle and multiple nozzle multi-material. For the tensile stress, Young's modulus, and tensile elongation, it was expected that the mechanical results of the specimen printed with both models would result in similar values mainly because the parameters used to 3D print were identical. However, the multiple nozzle extruder showed minor differences between the typical mechanical values in comparison to single polymer and single mixing nozzle extruder values. Examples of the multiple nozzle multi-material specimens printed are shown in Figure 4.8. The results show some defects in the boundary interface between materials. These defects could be caused by a formation of crystalline structures particularly in the edges of the polymer generating warpage and as a result a detachment from the build platform during the fabrication of the FDM part [21,22]. One of the factors was caused by parallax (user) error, mainly due to the calibration of the nozzles and could generate material shrinkage. Conversely, the multi-material

single nozzle demonstrated effective bonding between different materials (See Figure 4.9). It may be attributed to the single calibration needed for this model. As a result, the printing quality increased significantly in comparison to the multiple nozzle model. The proposed combinations of multi-material specimens that were tested and failed are shown in Figure 4.10.

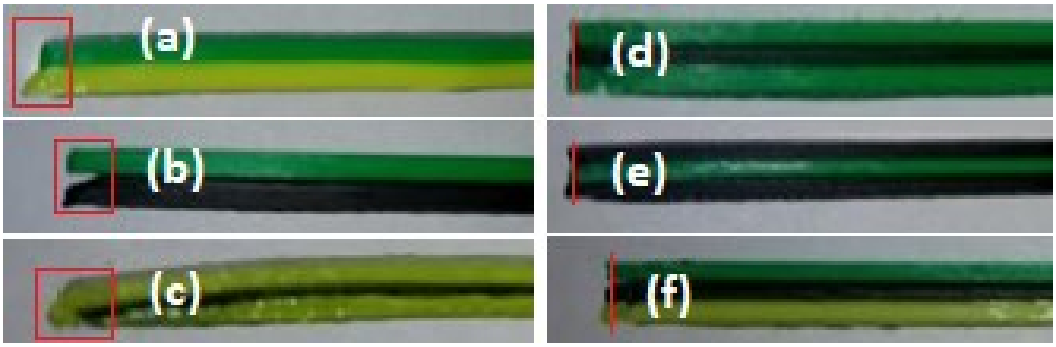

Figure 4.8 Defects on boundary interface (left) a) ABS-PLA, b) ABS-HIPS c) PLA-HIPS-PLA using the multiple-nozzle extrusion model

Figure 4.9 Effective bonding on boundary interface (right) d) ABS-HIPS-ABS, e) HIPS-ABS-HIPS, and f) ABS-HIPS-PLA using the single mixing- nozzle extrusion model

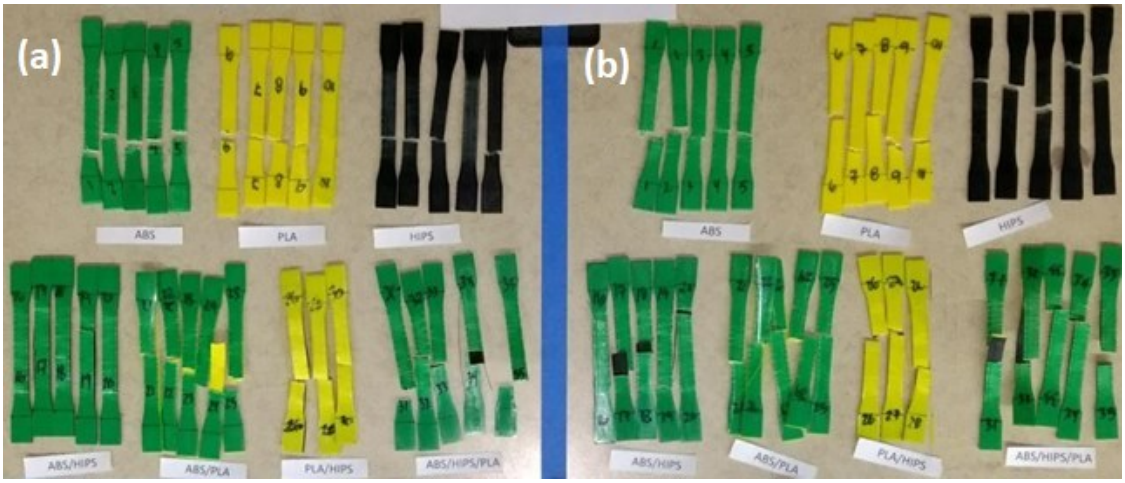

Figure 4.10 Failure of multi-material specimen a) multiple nozzles and b) single mixing nozzle

For build time and setup time- calibration, it was expected that a difference in time to build the part due mainly on the waiting time required (seconds) to reach extruder temperatures (transition time between different materials) would be identified. Additionally, the setup time - calibration difference was expected to be high because, for most of the components, bulkiness and wiring differ from each model.

The mechanical results are similar, considering that the specimen was printing with two different types of models. PLA and ABS demonstrated the highest tensile stress and Young's Modulus but a lower tensile elongation since they are considered rigid materials. On the other hand, the HIPS was among all the specimens, which showed the most moderate tensile stress and Young's Modulus.

Focusing on the different combinations and their physical boundary interface between materials, the results obtained were as expected when compared to a single material. Starting with the combination of the ABS-HIPS specimen, the tensile stress using the single mixing nozzle was within the same range (25.52 MPa) when compared to the multi-nozzle (25.36 MPa). In comparison with the original ABS (32.88 MPa), both models had lower values but with an increased amount compared to HIPS (20.06 MPa). Additionally, in terms of elongation, the single mixing nozzle (4.68 mm) was higher compared to the multi-nozzle (4.22 mm). In comparison with ABS (4.70 mm), the single mixing nozzle performed accurately, while the multi-nozzle possessed a lower value. Both models had a lower elongation compared to the original HIPS (5.74 mm). The Young's Modulus in the single mixing nozzle (1033.35 MPa), on the other hand, was higher than the multi-nozzle (1021.93 MPa). Both models displayed lower values compared to the ABS (1049.77 MPa) but showed higher values in comparison to the HIPS (947.67 MPa).

For the ABS-PLA specimen, the tensile stress using the single mixing nozzle was slightly lower (40.40 MPa) when compared to the multi-nozzle (41.70 MPa). In comparison with the original ABS (32.88 MPa), both models had higher values but a decrease value compared to PLA (47.45 MPa). Additionally, in terms of elongation, the single mixing nozzle (6.17 mm) was lower compared to the multi-nozzle (7.27 mm). In comparison with ABS (4.70 mm) and PLA (4.61 mm), both models displayed higher values (20 to 46% increment range). Furthermore, the Young's Modulus in the single mixing nozzle (1256.52 MPa) was within the same range of the multi-nozzle (1257.92 MPa). In comparison with the ABS (1049.77 MPa) and PLA (1396.90 MPa), both models had higher and within in range values. The performance of these two polymers demonstrated an effective bonding interface between both materials due to their compatibility with being rigid materials.

On the PLA-HIPS specimen, the tensile stress using the single mixing nozzle was slightly lower (29.60 MPa) when compared to the multi-nozzle (31.76 MPa). In comparison with the original PLA (47.45 MPa), both models had significantly lower values, but their performance was better compared to HIPS (20.06 MPa). Additionally, in terms of elongation, the single mixing nozzle (5.69 mm) was lower compared to the multi-nozzle (6.48 mm). In comparison with PLA (4.61 mm), both models showed higher values, but for the HIPS (5.74 mm), the single nozzle was slightly lower while the multi-nozzle had a higher value. Furthermore, the Young's Modulus in the single mixing nozzle (1027.08 MPa) was higher compared to the multi-nozzle (936.02 MPa). In comparison with the PLA (1396.90 MPa) and HIPS (947.67 MPa), both models had lower values.

For the ABS-HIPS-PLA case, the tensile stress using the single mixing nozzle was slightly higher (34.95 MPa) when compared to the multi-nozzle (33.78 MPa). In

comparison with the PLA (47.45 MPa), both models had significantly lower values. For the ABS (32.88 MPa) and HIPS (20.06 MPa), both models had a better performance. Additionally, in terms of elongation, the single mixing nozzle (7.56 mm) was higher compared to the multi-nozzle (6.53 mm). In comparison with ABS (4.70 mm), HIPS (5.74 mm), and PLA (4.61 mm), both models showed higher values (13 to 40% increment range). Furthermore, the Young's Modulus in the single mixing nozzle (1211.11 MPa) was higher compared to the multi-nozzle (1080.55 MPa). In comparison with the PLA (1396.90 MPa), both had lower values but higher compared to ABS (1049.77 MPa) and HIPS (947.67 MPa). This combination of three different materials makes it suitable when high stress and elongation is required for a specific application.

The results of all the combinations are summarized in Table 4.2, and column charts in Figures 4.11 - 4.13 are provided to view the comparison between models in their printing.

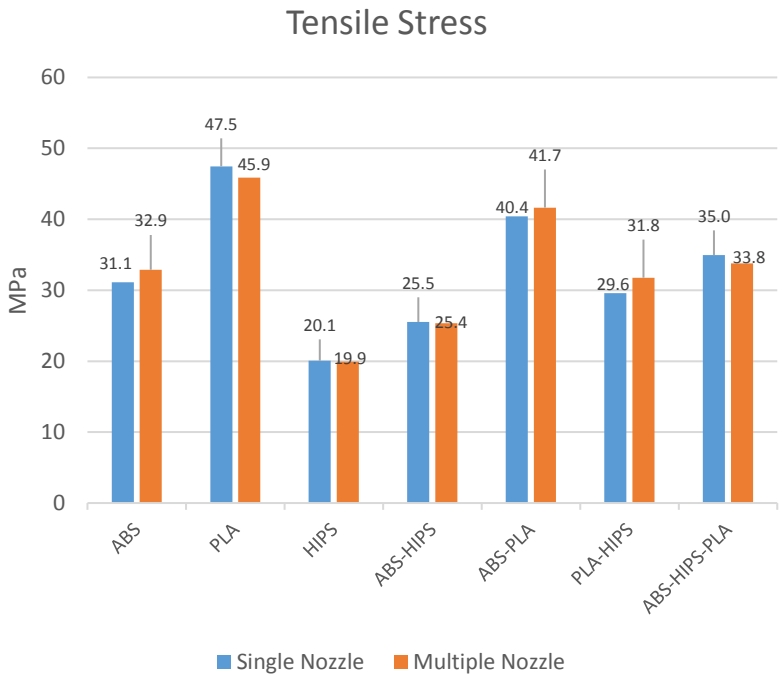

Figure 4.11 Mean tensile stress of all specimen tested

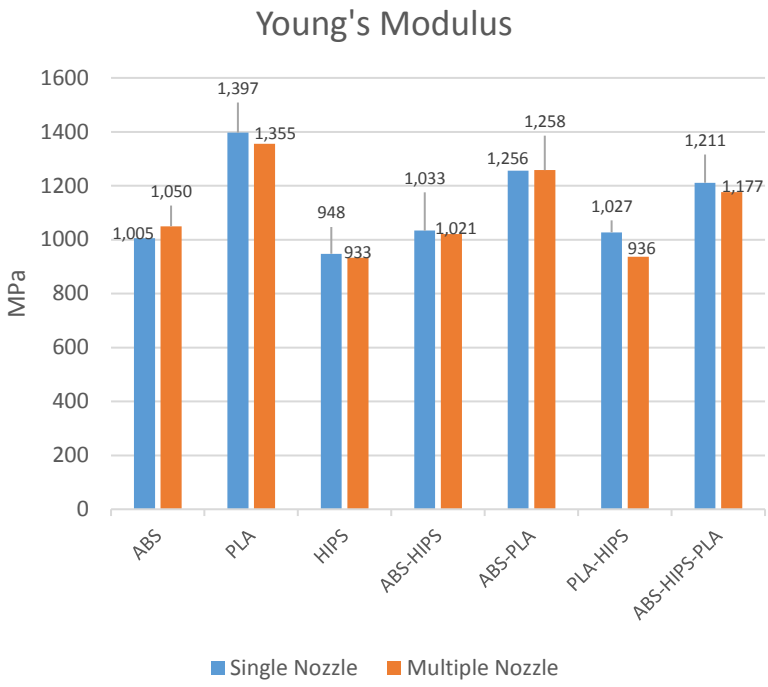

Figure 4.12 Mean Young's modulus of all specimen tested

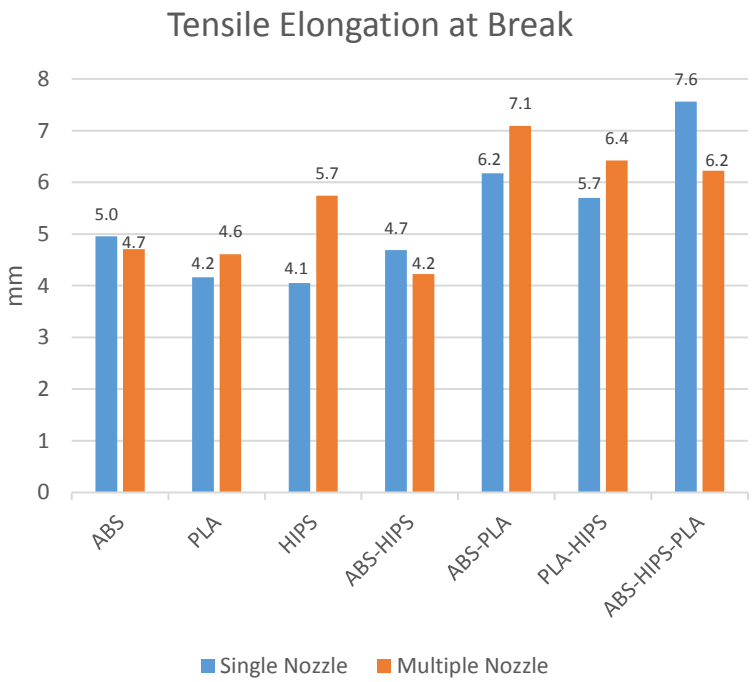

Figure 4.13 Mean tensile elongation at break of all the specimen tested

Table 4.2 Experimental results of multi-material specimens tested using both modes

Mode	Material	Tensile Stress (MPa)		Tensile elongation at break (mm)		Young's Modulus (MPa)		Build time (min)	
Nozzle	**Combination**	**Mean**	**StdDev**	**Mean**	**StdDev**	**Mean**	**StdDev**	**Mean**	**StdDev**
Single Mixing Nozzle	ABS-HIPS	25.52	0.14	4.69	0.77	1033.36	8.18	50.31	0.14
	ABS-PLA	40.4	1.57	6.17	1.28	1256.43	107.18	48.75	0.11
	PLA-HIPS	29.6	0.79	5.7	0.74	1027.08	23.78	49.59	0.23
	ABS-HIPS-PLA	34.95	0.17	7.56	1.47	1211.12	6.77	52.29	0.11
Multiple Nozzle	ABS-HIPS	25.36	0.06	4.22	0.31	1021.4	8.35	48.23	0.02
	ABS-PLA	41.7	0.44	7.09	0.73	1257.93	84.6	48.35	0.02
	PLA-HIPS	31.77	1.74	6.48	0.86	936.02	245.76	48.26	0.02
	ABS-HIPS-PLA	33.79	1.36	6.53	0.62	1080.56	48.87	48.51	0.07

The capabilities of each model, the single nozzle multi-material, performed accurately in the machine regardless of the type of polymer implemented. The interface layer bonding between materials was sufficient to fabricate the multi-material specimen accordingly to the strategy proposed. This model has the advantage of printing multi-functional components by improving its mechanical properties. Thus, it can be used to reinforce crucial segments where a specific load may be applied. To achieve the potential of this mode, a strong understanding of the geometry of the nozzle and parameters of each polymer is required. Otherwise, difficulties may appear when extruding material from the single multi-material nozzle. These include jamming, material contamination and, finally, a reduction in the quality of the final part. Additionally, this model is capable of working with functionally graded materials, i.e., when a part requires a mixing percentage ratio

with similar or different materials, manufacturing lightweight components and implementing topology optimization [60] within a critical part.

On the other hand, the multiple-nozzle encountered some problems that were mainly technical factors such as the nozzle calibration and precision of enabling each hot end extruder at a time. Consequently, some 3D printed specimens displayed higher delamination in their boundary interface when switching between materials. In terms of efficiency and quality, this model was too bulky and lacked precision when handling several nozzles (caused mainly by parallax-error to level each nozzle accurately).

For this reason, a collision can occur between a nozzle and a printed layer. With an adequate calibration or even by implementing an automatic switch leveling, the advantages increase significantly. A time reduction may be noticed when printing several components in a single time frame, or even print as a mass production perspective and as well as the elimination of any possible material contamination

To define a suitable model based on previously collected data from the tensile tests, a comparison matrix is shown in Table 4.3. It reflects the limitations and advantages encountered during the implementation of each technology. The limitations of this study were that the 3D printer could handle only three extruders; therefore, three materials can be used at a time. Additionally, the specimens were printed as a stack of different material layers in the same section. In future work, it is intended to add an external controller to expand the capabilities of more extruders. Moreover, studying functional gradient materials utilizing different polymers and evaluating composite materials where strength reinforcements and lightweight components are necessary for the additive manufacturing sector.

Table 4.3 Comparison to select the best manufacturing process based on the final product performance between single mixing nozzle and multiple nozzle extrusion

Conditions	Multi-material Nozzles Comparison	
	Single Mixing Nozzle	**Multiple Nozzles**
Quality		
Nozzle oozing/ string	Minimum	Control of pressure for disabling idle nozzles while printing
Color mixing	Color and material gradient	N/A (material combination)
Contamination	Material control deposition flow	Requires to control idle nozzles to prevent polluting the print
Material Waste	Purge needed/ prime nozzle	Minimum
Temperature		
Nozzle Temperature	Single heater cartridge	Separate heater cartridges per nozzle
Thermistor Sensor	Single thermistor	Separate controlled thermistors per nozzle
Cooling System	Mostly fan-cooled system	Fan or Water cooled system
Calibration		
Nozzle Offset	Single calibration	Not perfectly calibrated
Layer Height	Single time alignment	Not perfectly aligned
Retraction	Additional retraction forces are generated based on the internal geometry	Same retraction values for the number of nozzles used
Extrusion		
Filament	Single diameter size exit hole	Multi- nozzles, multiple diameter exit holes
Jamming	Backflow of molten filament	Minimum, control pressure

4.6 Conclusion

This paper has demonstrated the capabilities and drawbacks of two existing multi-material FDM nozzle models. The main issues of which technology is suitable for different bond polymers within the same geometry/section were addressed. Their working principle of extruding material is relatively similar; however, when switching or combining different materials, a boundary interface will always be generated with both models.

This study analyzed the complexity of these models at three stages: Firstly, it evaluated the performance of printing standard specimen using a single multi-material nozzle extrusion and a multiple-nozzle extrusion nozzle. Secondly, it collected data from the tensile test of the printed samples to demonstrate which model was able to generate feasible and reliable properties between the multi-material specimens. Lastly, it showed a summary of the main characteristics of both models based on their performance and advantages.

In terms of the mechanical properties between both modes, there was a minor difference of less than 5% in their values. The multi-nozzle demonstrated a better performance in the build time but encountered minor issues calibrating the nozzles. On the other hand, the single nozzle displayed greater consistency in generating better quality materials and is, therefore, a better option to be used to fabricate gradient materials. Overall, this paper mainly studied the multi-material filament extrusion models used for conventional polymer materials. The use of multi-materials can lead to improvement to fabricate functional parts, and effectively, increase mechanical properties. In the next chapter, a new scheme of sandwich structure using conventional 3D printing materials is presented. Tensile experiments were conducted to identify an improvement in their mechanical properties by combining different materials when compared to single homogeneous materials.

Chapter 5
Tensile mechanical behaviour of multi-polymer sandwich structures via fused deposition modelling

5.1 Introduction

Additive manufacturing (AM) has represented a robust manufacturing development and process of design for products in a wide variety of sectors, including aerospace, biomedical, and manufacturing [61]. AM technology can fabricate accurately and strengthened components in a fast production, being able to either be combined with traditional manufacturing techniques known as hybrid technologies, i.e., subtractive and additive remanufacturing [62,63] or even as an option to displace them shortly [64]. Presently, extensive research on fused deposition modelling (FDM) materials is being carried out on thermoplastic polymers and composites due to their cost-effective, lightweight, and high strength-to-weight ratio [29]. Material selection methodologies have been developed to choose optimal materials at the early design stages of the AM processes [65]. Some research is done by combining materials including, polylactic acid and polycarbonate (PLA-PC), acrylonitrile butadiene styrene and polycarbonate (ABS-PC), and polyethylene and polypropylene (PE-PP) [5].

In recent years, the fabrication of multi-material polymer-based products and sandwich structures methods applied to the FDM process has brought the attention

of the industry and research community. The benefits of multi-material applied to smart components enable the performance of shape memory polymers by improving 3D printing quality through topology optimization of different process parameters [60,66]. Thus, producing multi-material components may enhance the mechanical properties, enable new functionality, and improve the performance of the AM process. [27]. Besides, sandwich structures made of different polymers combinations have been considered an excellent option to achieve various material properties for customized products [67], i.e., light-weight interior components in the automotive sector. Usually, sandwich structures are applied to composite materials, which consist of outer skins (thin facings) made of high-strength material sandwiching the inner core made of a lightweight material [68]. The inner core usually consists of a honeycomb configuration due to its weight efficiency. However, it can encounter problems such as water intrusion and delamination [69]. Daniel and Abot [70] suggested that by varying the materials for the skin and core can enable the desired stiffness and strength. Herranen et al. [71] concluded that the optimal design to develop a light-weight sandwich composite appears to be more accurate in the core material than in the core layer thickness. For homogenous thermoplastics on the FDM process, Lanzotti et al. and Chacón et al. [72,73] studied the influence of the process parameters (layer thickness, flow rate, deposition speed, feed rate, and build orientation) for single specimens made of PLA. The first author concluded that all the fibers had to be oriented along the loading line to maximize the value of Young's modulus and stiffness. The second author realized that on- edge samples (build orientation) showed the best performance in terms of strength, stiffness, and ductility. Also, as the layer thickness and feed rate is increased, ductility is decreased. Fernandez-Vicente et al. [74] evaluated the strength of different mesostructures for

ABS manufactured with the FDM process. For the evaluation, a tensile test was conducted with various parameters including the material densities and infill patterns to select the optimal specimen. The best combination to obtain the highest tensile strength was the rectilinear 45° pattern with a 100% infill density. Qureshi et al. [75] proposed a decision –matrix method with a set of 13 parameters for FDM to assess and identify the effect on the mechanical properties of ABS. He conducted an experimental tensile test to identify the influence factors on the ultimate tensile strength (UTS) and elastic modulus with Taguchi's method for the design of experiments and analyzed the obtained parameters accordingly. Heechang [76] discussed the use of single and dual materials for the development of multi-material printing. The paper proposed the influence of equipment variables, material ratio percentage and different structural arrangements to identify and improve the mechanical behavior of the specimens. Lopes et al. [47] examined the effect of the boundary interface formed in different zones using dual nozzles to fabricate multi-material parts. The tested specimens showed a decrease in their tensile strength and Young's modulus due mainly to switching between extruders. The author suggested that a proper design for the boundary interface must be implemented to achieve higher mechanical properties. Singh et al. and Kumar et al. [25,46] conducted mechanical tests to find the best material combination between ABS, PLA, and HIPS. The three materials were printed in the same geometry as a stack of different multi-layers, and the twin extrusion method (TSE) was implemented. The proposed study was influenced by the infill percentage and printing speed of each material combination. Saad [77] fabricated a sandwich structure with ABS and PLA to test the variation of their mechanical and physical properties. The study consisted of different infill percentages of honeycomb cores to identify the effect of pore size

volume on the mechanical properties and to validate the weight benefit. The results of the tensile and bending test showed that the tensile strength increases as long as the infill density increases while the stiffness remains constant with bending stress. Brischetto et al. [78] proposed a three and four-point bending tests for ABS and PLA using sandwich structures. The proposed experimental analysis was influenced by the infill patterns (honeycomb and homogenous) as core layers and by the number of extruders (two) to fabricate the specimens. All these parameters had a significant influence on their modulus of elasticity especially in those specimens made of ABS skins and PLA honeycomb core. Santosh et al. [79] prepared multilayers structures using ABS with PLA to find out an improvement on their mechanical behaviour. The mechanical properties were evaluated using the tensile test, compressive test, bending test, microhardness and surface roughness. De Souza et al. [28] studied the mechanical properties of blending ABS and HIPS to analyze the effect of shot size and particle size via injection molding. The results suggested that increasing ABS in the ABS/HIPS blend leads to an increase in the tensile strength and Young's modulus, but it decreases the elongation at break. Dinesh et al. [80] investigated the mechanical properties of a sandwich structured CFRC with different combs such as aluminum honeycomb, Rohacell, and HDPU foam core. The tensile results observed that the aluminum honeycomb core could easily tear in axial loading compared to the rest; however, for the bending test, it presented the highest bending load among the other materials. Galatas et al. [81] proposed to enhance the mechanical properties of composite sandwich structures for ABS with carbon fiber reinforced polymer (CFRP). The parameters considered in the study were the infill densities and the number of CFRP layers. The ultimate strength of these composite dog-bone specimens was evaluated, employing a tensile test. The experimental results were

compared with a developed artificial intelligence neural network, and the influence of other properties such as Young's modulus and specific strength was also discussed.

In the authors' previous work, tensile tests for single material specimens made of PLA [72,73], and ABS [74] were conducted. The proposed methodologies using image analysis and statistical analysis were used to evaluate the mechanical properties (tensile strength, tensile strain, and elastic modulus) of the produced samples following the ASTM 638 type. Besides, most of the experimental tests employed for the sandwich structures in the past were conducted by considering the ASTM D790 and the ASTM D6272 standards for flexural properties of un-reinforced and reinforced thermoplastics, respectively. Based on the literature review and to the best of the authors' knowledge to date, the use of sandwich structure applied to different combinations of materials via FDM for improving the mechanical properties is lacking, which is the aim of this paper.

The present paper investigates and tests the influence of sandwich structures applied to conventional 3D printing materials to improve the mechanical properties of 3D printed prototypes. The new sandwich structure here proposed are specimens embedding rectilinear cores pattern with a 100% infill density and applying multiple independent nozzle extruders for each material within the same carriage. This new scheme could provide a piece of knowledge for comparison on the effect of combining conventional materials (ABS, PLA, and HIPS) as a sandwich structure to achieve and enhance higher strength of polymeric parts, which can be used for various applications, i.e., unmanned aerial vehicles (UAV). The tensile experiments aimed to identify whether the use of conventional materials printed as a sandwich structure is suitable and beneficial to implement and able to improve their mechanical behaviour (tensile strength, elongation at break, and Young's modulus) when

compared with a single material 3D printed part. Therefore, the contribution of this paper lies in finding the best final product performance of the selected materials.

5.2 Materials and Methodology

The first material selected for this study was PLA. It is widely used in FDM 3D printing [82] and provides some benefits against other polymers such as environmentally friendly material, sustainable, biocompatible, and has excellent plasticity in the long term use [23]. The second material implemented is ABS. For the extrusion process, ABS provides excellent heat and high resistance, low thermal conductivity, toughness, and compatibility with other materials [19]. Lastly, high impact polystyrene (HIPS) present high impact strength and low tensile strength and provides simplicity for its fabrication and machinability [25].

5.2.1 Process Parameters

For this study, it was aimed to enhance the strength of a part by investigating the effect of different material sandwich arrangements in the same geometry. The method proposes a sandwich structure with a total thickness of 3.6-mm. The two outer skins have a global thickness of 2.4-mm and the inner core a thickness of 1.2-mm made of a different polymer with a rectilinear infill pattern and 100% density. The materials used to manufacture the test specimens were spools of 1.75 mm diameter of ABS, PLA, and HIPS. The mechanical properties of these materials are reported in Table 5.1 [26]. The filaments were obtained through the same commercial supplier. The specimens were fabricated following the D638- Type 1 standard [53] to analyze how the structural arrangement determines a change in their tensile strength. Firstly, specimens were printed as a single homogeneous material with fixed parameters to be compared with the multi-material specimens. Secondly, the combination of

materials for the sandwich structure was performed with four layers section of each material. The material configurations to fabricate the sandwich structure specimen are shown below. Figure 5.1 illustrates the specimen designs for homogeneous materials and sandwich structure material combinations. In addition, the printed parameters carried out to print the specimens are summarized in Table 5.2. The main dimensions of the specimen are shown in Figure 5.2.

- PLA-ABS-PLA and PLA-HIPS-PLA
- ABS-PLA-ABS and ABS-HIPS-ABS
- HIPS-PLA-HIPS and HIPS-ABS-HIPS

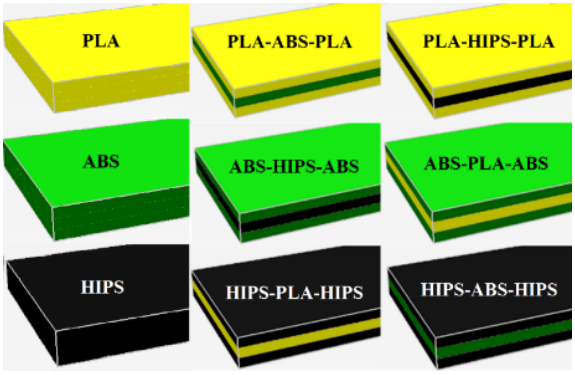

Figure 5.1 Geometry for a typical specimen as a single material and as a sandwich structure part (three-layer section with equal thickness)

Table 5.1 Typical mechanical properties of ABS, PLA, and HIPS

Material	**Polylactic Acid (PLA)**	**Acrylonitrile Butadiene Styrene (ABS)**	**High Polystyrene (HIPS)**	**Test Method**
Tensile Modulus (MPa)	890 to 3647	1697 to 2826	1565 to 2290	ASTM D638
Tensile Strength (MPa)	17.6 to 64	32 to 53	20 to 31	ASTM D638
Tensile Strength Yield (MPa)	15.5 to 72	29 to 57	16.4 to 30	ISO 527-2
Tensile Strength Break (MPa)	13.7 to 70	15 to 50	16 to 30	ISO 527-2
Tensile Elongation Yield (%)	9,8 to 10	2.0 to 21	4.0 to 61	ASTM D638
Tensile Elongation Break (%)	0,50 to 19	0.90 to 57	27 to 63	ASTM D638
Flexural Modulus (MPa)	2275 to 4495	1420 to 2770	1372 to 2454	ASTM D790
Flexural Strength (MPa)	57.6 to 109	44.6 to 89	20.6 to 64.6	ASTM D790

Table 5.2 Printing parameters

Infill pattern	**Rectilinear**
Infill speed (mm/s)	25
Travel speed (mm/s)	100
Retraction speed (mm/s)	5
Infill density (%)	100
Flow rate, %	100
Infill angle	45°
Thickness (mm)	0.3
No. of perimeters	3
Bed temperature, °C	90
Nozzle temperature, °C	240

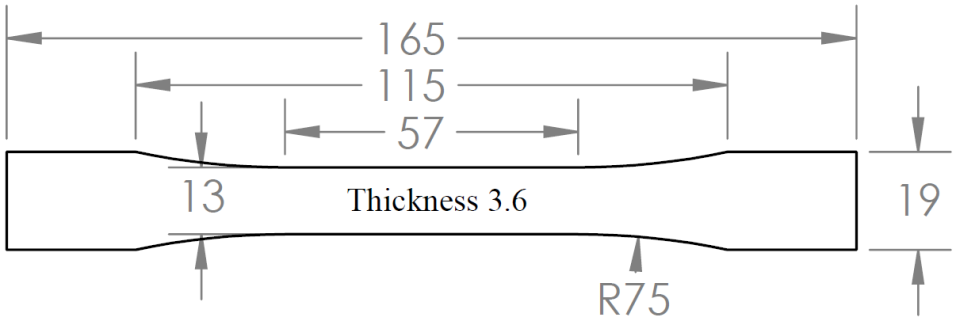

Figure 5.2 Standard test specimen in mm

5.3 Experimental

For the present study, a multi-material 3D printer was developed and customized to allow the use of multiple filaments. It was necessary to integrate a multiple- nozzle head extruder to enable producing different materials. The extrusion unit consisted of four nozzles within the same carriage. The module is based on the Bowden extrusion system [35], where the extruder mechanism is away from the printer's heated head. The hotend of the extrusion nozzle integrated a water-cooled channel that serves as a heatsink to keep it continuously cooled while printing. The nozzles

used on this module had a die diameter of 0.4 mm each. It was necessary to find the exact distance (height and width) and offset values between each nozzle to ensure that once it deposits material, an overlap between layers exists (See Figure 5.3). The nozzle levelling was carried out using a capacitive sensor, which was enabled in the Z-axis. Figure 5.4 shows the multi-nozzle extruder with the sensor and the specimens while printing.

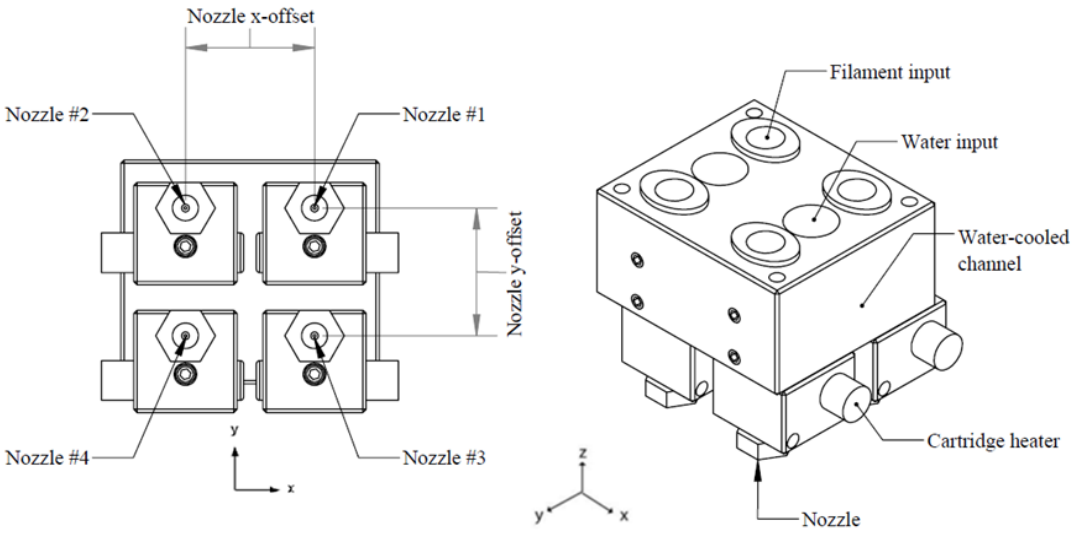

Figure 5.3 Illustration of the multi-nozzle module bottom side with the X-Y offsets (left) and isometric view (right)

The machine used to perform the tensile tests was the Instron 5966. It was configured with a minimum speed of 2 mm/min, a load cell of 10 Kn, and a gripper with a maximum load of 5 Kn. The specimens were loaded along the longitudinal axis until failure. According to the standard and for the evaluation of dispersion, five specimens were printed for each material configuration. A total of 45 specimens were printed to validate the results.

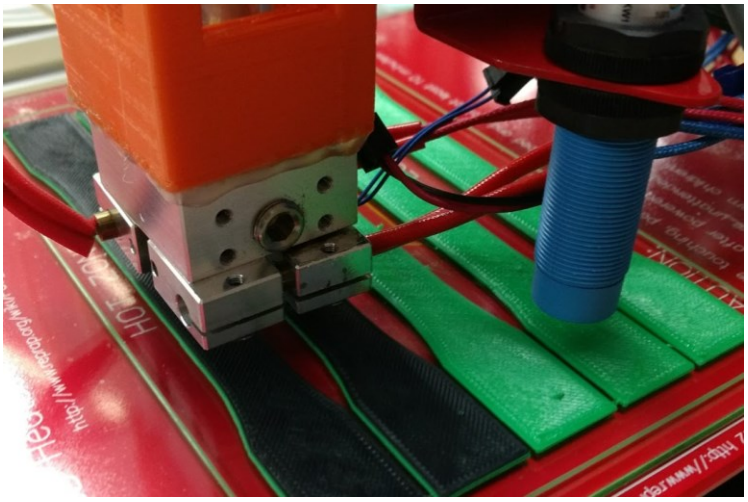

Figure 5.4 Multi-nozzle extruder while printing ABS-HIPS-ABS specimen

5.4 Results and Discussion

This section addresses the effects on the mechanical properties of all samples. The mechanical properties considered for the comparison were the tensile strength, tensile elongation at break, and Young's modulus.

The mechanical results obtained from the tensile test show differences between the homogeneous materials and the different combinations of sandwich structures. To evaluate the dispersion of the tests, results are shown in the next figures. Figure 5.5 shows the tensile strength results according to the different material combinations, and Figures 5.6 and 5.7 show Young's modulus and tensile elongation at break with the same configuration as the previous figure. Specimens printed as a single material such as PLA and ABS showed a higher ductile response when compared to the other specimens. PLA demonstrated the highest tensile strength (47.46 MPa) and Young's modulus (1396.90 MPa) among all specimens but presented the lowest elongation at break (4.16-mm). HIPS exhibited plastic deformation and showed the lowest tensile strength (20.06 MPa) and Young's

modulus (933.33MPa) but had a higher elongation at break (6.69-mm) when compared to these two. Moreover, it was expected that the performance of combining different materials would have a positive impact on the mechanical properties in comparison to the single material ones. In general, three types of specimen showed higher ultimate strength and elastic modulus when fabricated with the sandwich configuration than compare to a single material. Among these specimens, the combination of PLA-ABS-PLA had the best tensile strength and Young's modulus with a mean of 44.40 MPa and 1364.57 MPa, respectively. This behaviour may be due that both polymers are considered rigid materials. Secondly, PLA-HIPS-PLA had slightly higher tensile strength, and Young's modulus (38.77 MPa and 1351.27MPa) compared to ABS-PLA-ABS with a tensile strength of 38.28 MPa and Young's modulus of 1232.96 MPa. Also, the highest elongation at break exhibited from these three specimens was 6.14-mm from the PLA-HIPS-PLA sandwich structure.

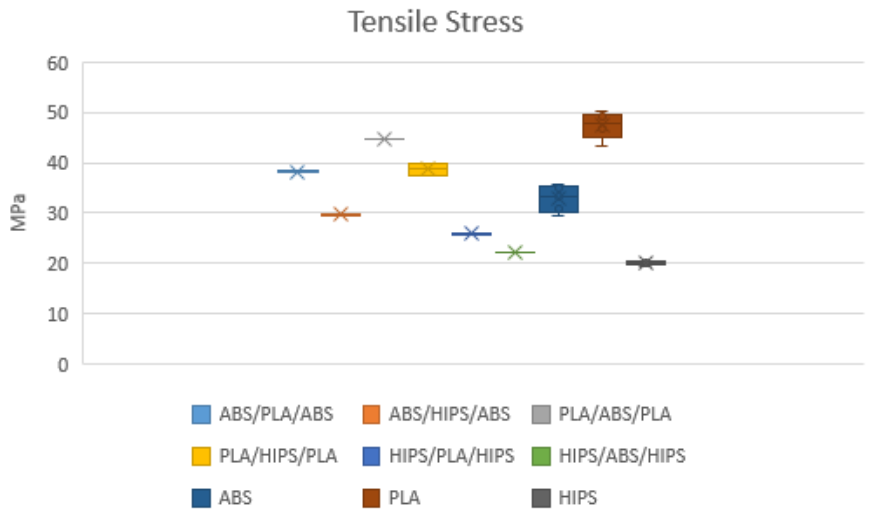

Figure 5.5 Mean tensile stress of all specimen tested

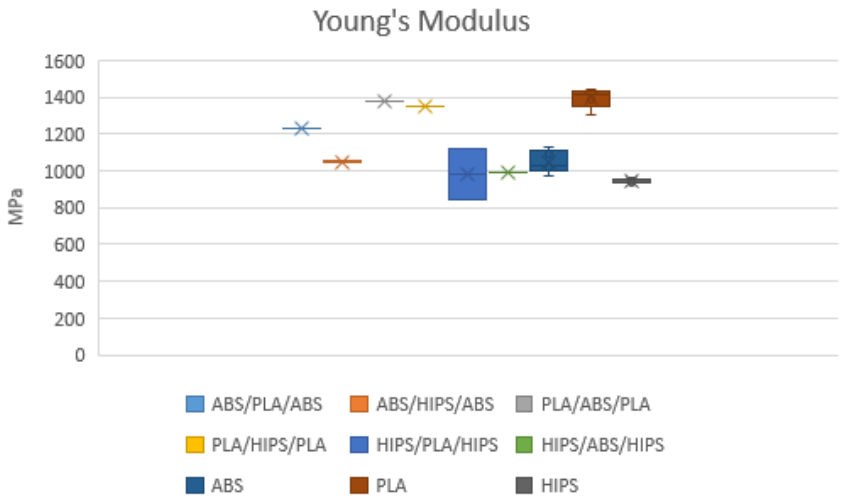

Figure 5.6 Mean Young's modulus of all specimen tested

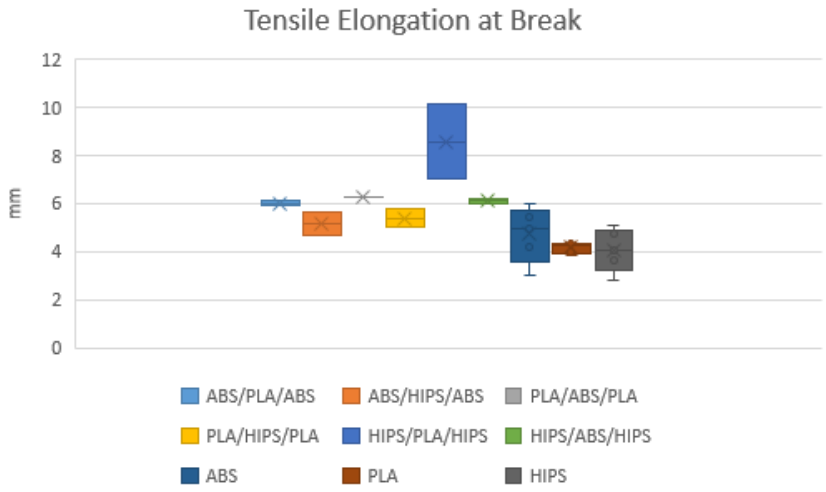

Figure 5.7 Mean tensile elongation at break of all specimen tested

Figures 5.8 and 5.9 show representative examples of the tested specimens illustrating the failure mode. In Figure 5.8, the fracture in all specimens shows the different stress distributions of the material combinations. It can be seen by comparing D, G, and H specimens that the fracture reveals the cracking pattern

generated closely to failure. Figure 5.9 show that most of the fractures on the sandwich structures started on the skin layers, followed by the failure in the core materials. This type of failure occurs when layer delamination and higher stress between the different materials is presented.

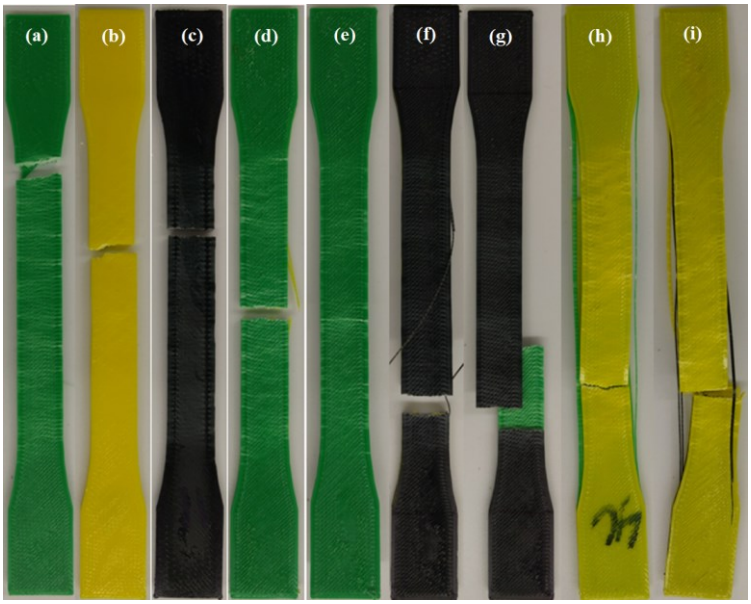

Figure 5.8 Examples of tested specimens a) ABS b) PLA c) HIPS d) ABS-PLA-ABS e) ABS-HIPS-ABS f) HIPS-PLA-HIPS g) HIPS-ABS-HIPS h) PLA-ABS-PLA i) PLA-HIPS-PLA

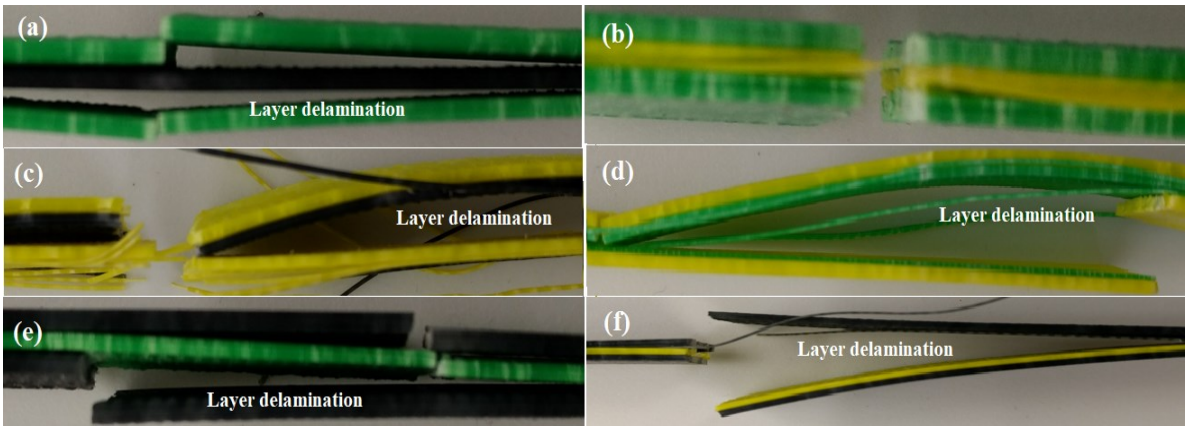

Figure 5.9 Detail view of fractured specimens printed as a sandwich structure a) ABS-HIPS-ABS b) ABS-PLA-ABS c) PLA-HIPS-PLA d) PLA-ABS-PLA e) HIPS-ABS-HIPS f) HIPS-PLA-HIPS

Figure 5.10 compares the stress-strain curve of all the specimens. The analysis shows that the specimens at the beginning of the test experimented with a linear trend surpassing the stress of 15-20 MPa. Consequently, this trend changed considerably in different stages for each specimen when the ultimate strength was reached. The specimens with HIPS skins and ABS rectilinear core presented the worst performance with a mean tensile stress of 22.21 MPa and Young's modulus of 992.02 MPa, which is less than 50% and 28% respectively when compared to the best sandwich structure tested which was PLA-ABS-PLA. Similar behaviour was encountered with the specimens with HIPS skins and PLA core. They showed a low mean tensile strength of 25.87 MPa and Young's modulus of 981.45 MPa but performed better when reaching the highest elongation of all with a mean of 8.57-mm.

The infill fibres of the skin layers deform rapidly and absorb the stress-causing to break the bonds within materials. Failure across the interface of materials can be observed. The bonding zones between each layer section correspond to the previous layer material where delamination occurred. The location of the ruptures of the sandwich- structured specimens were mostly generated near the jaws of the test equipment. In addition, the fractures occurred as a consequence of the boundary interface between materials. It can be concluded that these interfaces are the weakest regions when building a sandwich structure with multiple materials. Despite this condition, using a sandwich structure arrangement for conventional materials can improve the mechanical properties as demonstrated and described previously. The generated matrix of the corresponding results of the different sandwich structures is shown in Table 5.3. The data listed in the table confirm the results obtained from the box plot graphs and the stress-strain diagram.

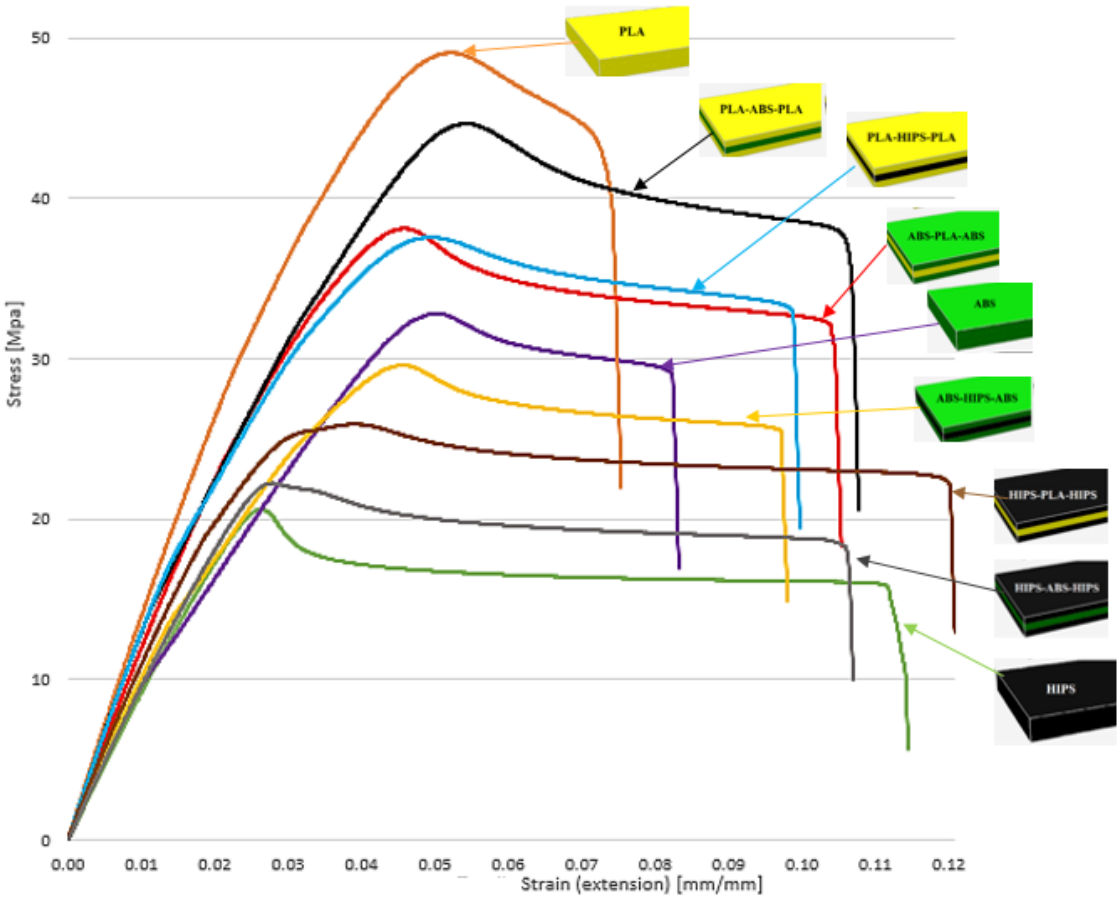

Figure 5.10 Stress-strain curve diagram of all the specimens tested

Table 5.3 Results on the stress-strain response homogeneous and sandwich-structured specimens

No	Material(s)	Tensile stress (MPa)		Tensile elongation at break (mm)		Young's Modulus (MPa)	
		Mean	StdDev	Mean	StdDev	Mean	StdDev
1	ABS	32.89	2.32	4.71	1.03	1049.78	54.81
2	PLA	47.46	2.37	4.16	0.20	1396.90	47.33
3	HIPS	20.06	0.26	6.69	1.92	933.33	14.69
4	ABS-PLA-ABS	38.28	0.16	6.02	0.07	1232.96	0.78
5	ABS-HIPS-ABS	29.67	0.07	5.16	0.52	1049.05	4.87
6	PLA-ABS-PLA	44.40	0.26	6.14	0.09	1364.27	16.68
7	PLA-HIPS-PLA	38.77	1.18	5.38	0.38	1351.27	2.50
8	HIPS-PLA-HIPS	25.87	0.06	8.57	1.56	981.45	141.42
9	HIPS-ABS-HIPS	22.21	0.05	6.10	0.12	992.02	3.59

5.5 Conclusion

This research presented a unique polymer-based sandwich structure to evaluate the tensile properties of different material combinations produced via the FDM process. The aim of the paper was applied to the fabrication of rectilinear infill cores and outer skins of several materials via multiple nozzle extruders. Experimental findings in the 3D printing process showed that the best sandwich-structured arrangement was the combination of outer skins of PLA and ABS cores. The average values were 44.40 MPa for the tensile strength and 1364.25 MPa for Young's modulus. Also, the elongation at break (6.14-mm) for this configuration was higher when compared to an homogeneous material. Specimens with outer skins of HIPS and ABS cores showed the lowest performance compared to the rest sandwich specimens. The mechanical behaviour of the sandwich structures is different compared to a single material. The change of the material arrangement determines mainly the tensile strength, elongation at break, and stiffness between 30% and 50%. Ultimately, this paper demonstrated the capabilities and flexibilities of conventional 3D printing materials to be used to improve the efficiency of an AM product. Therefore, the use of the sandwich structure applied to conventional 3D printing materials can increase the durability and robustness over single homogenous materials by integrating the properties of two materials in the same part. It also can provide higher elongation at break, which can absorb energy and therefore give long-term use before failing. The advantages of multi-material and sandwich structures methods are suitable to implement and able to achieve the requirements of various applications using low-cost materials.

Chapter 6
Conclusion

6.1 General conclusion

The additive manufacturing of multi-material parts has become a convenient solution to generate complex and specialized parts with customized materials and properties. However, it can be a complicated process to build multi-material parts in a practical scenario. Therefore, in this thesis, an FDM system was developed at LIMDA for the fabrication of multi-material thermoplastic polymers. The system hardware consisted of a motion control subsystem, which was integrated by the X-Y-Z axes linear actuators and a multi-material deposition subsystem with three extruder stepper motors for the different types of materials. It was successfully designed to be flexible and reconfigurable which is the main contribution of this research. The system supports the combinations of multi-material nozzles extrusion technologies that can produce either graded materials using a mixing nozzle or as a combination of different types of materials in the same geometry using a multi-nozzle extruder. One central control unit is implemented for controlling both subsystems. Once the path planning is generated in the slicing process, machine instructions are generated in a G-CODE format. With these instructions, the system was able to execute them and therefore run the actual moving process. All the components and software implemented in this work are open-source platforms, which gave research to explore in a free of use. To fabricate and to evaluate the multi-material parts in the actual system, several approaches are considered: Firstly, combinations of different types of materials are placed on top of each other with a simple contact interface and with a specific layer

thickness using multi-nozzle extruders and mixing nozzle extruders. Secondly, parts are produced within any given layer with the use of a mixing print head nozzle giving the effect of a graded component. Some parts were designed in CAD software and split into different sections to fabricate the final part, and others are designed as a single model, but the percentage ratio of material deposition was modified in real-time while printing. All fabricated multi-material specimens were subjected to a controlled test using a destructive tensile test process to obtain information on their tensile strength, elasticity, and elongations at the break. The collected information helped understand the behaviour of combining different materials in the same section and able to identify among them the best sandwich-structured arrangement on conventional 3D printing materials.

6.2 Research contributions

The contributions of this research can be summarized as follows:

- Experimental setup and development of an FDM system to produce multi-material polymers with two different extrusion material modes.
- A comparison of single mixing nozzle and multiple nozzles for the FDM to select the best manufacturing process technology based on the final product performance.
- An experimental evaluation to identify the tensile mechanical properties of specimens printed as multi-material parts.
- An experimental investigation of the influence of sandwich structures applied to conventional 3D printing materials by implementing a new sandwich structure scheme.

6.3 Research limitations

This research is subject to the following limitations:

- The accuracy of the developed software is not optimal at this stage and requires further work for the integration of the multi-material process.
- The system has proved its functionality to 3D print multi-material specimens but has to be validated with a real case study.
- It is only limited to print three materials simultaneously; therefore, to extend its capabilities of more materials, external control devices needed to be integrated.

6.4 Proposed future research

The proposed future research is illustrated in Figure 6.1 and described as follows:

- Apply topology optimization to FGM for multi-material FDM fabrication.
- 4D Printing is a new process in AM capable to transform over time the shape of a material to another directly off the print head. In the future, a design and implementation of a new print head that can handle different types of materials such as composites, nanoparticles addition and advanced smart materials will be presented to produce functional folding applications.
- Integrate a machine learning vision system as a supervisory quality control feedback loop to monitor in real-time each multi-layer and detect/fix defects such as void, over-fills, and under-fills.

- Enable into this multi-material extrusion system, other manufacturing technologies, i.e., molding, subtractive, to create an intelligent hybrid solution.

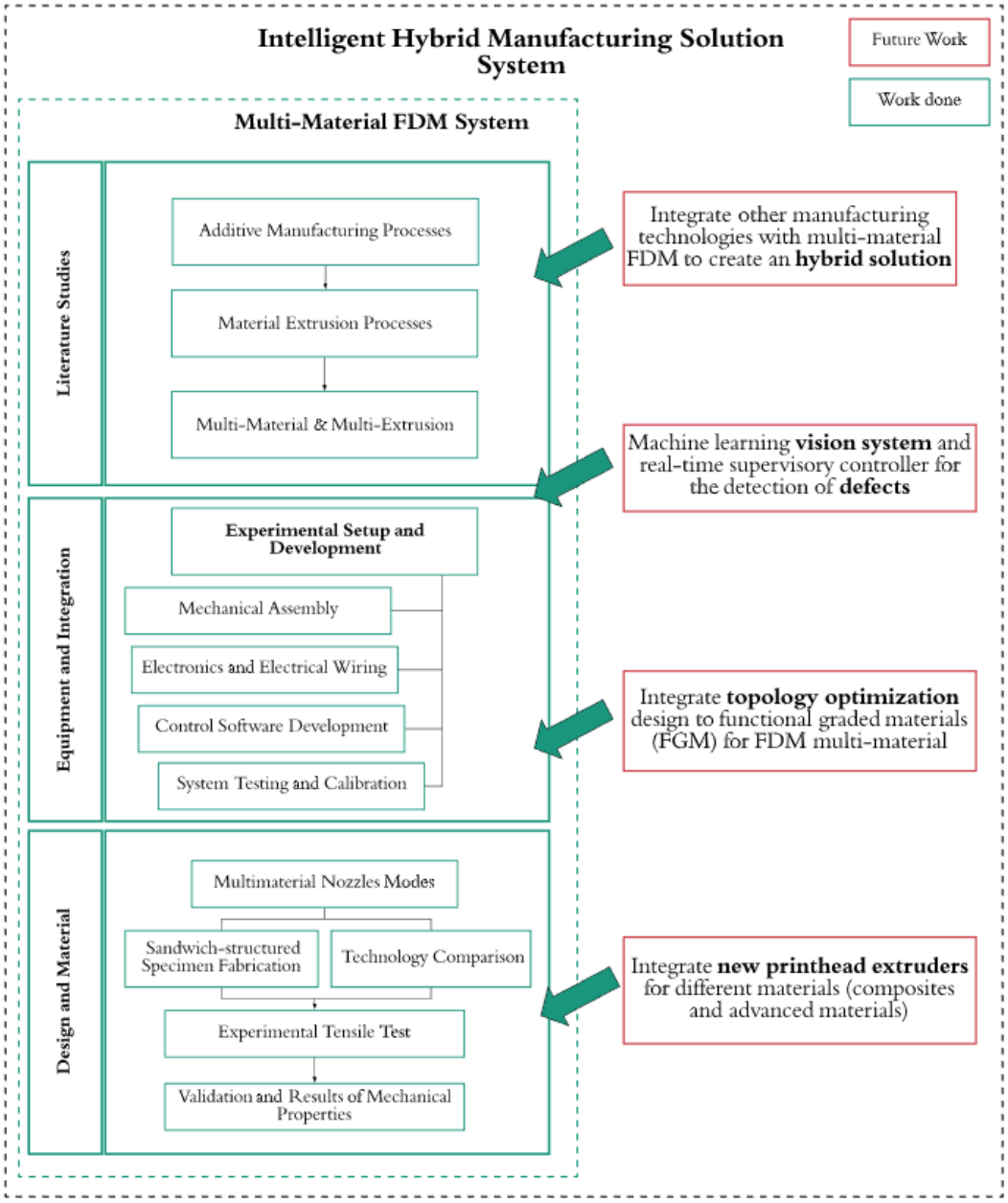

Figure 6.1 Future research path

References

[1] Gebhardt, A. and Gebhardt, A. (2011) Basics, Definitions, and Application Levels. *Understanding Additive Manufacturing*, 1–29. https://doi.org/10.3139/9783446431621.001

[2] Gebhardt, A., Hötter, J.-S., Gebhardt, A. and Hötter, J.-S. (2016) Characteristics of the Additive Manufacturing Process. *Additive Manufacturing*, 21–91. https://doi.org/10.3139/9781569905838.002

[3] Gonzalez-Gutierrez, J., Cano, S., Schuschnigg, S., Kukla, C., Sapkota, J. and Holzer, C. (2018) Additive manufacturing of metallic and ceramic components by the material extrusion of highly-filled polymers: A review and future perspectives. *Materials*, 11. https://doi.org/10.3390/ma11050840

[4] Gebhardt, A., Kessler, J., Thurn, L., Gebhardt, A., Kessler, J. and Thurn, L. (2018) Basics of 3D Printing Technology. *3D Printing Understanding Additive Manufacturing*, p. 1–32. https://doi.org/10.3139/9781569907030.001

[5] Mohan, N., Senthil, P., Vinodh, S. and Jayanth, N. (2017) A review on composite materials and process parameters optimisation for the fused deposition modelling process. *Virtual and Physical Prototyping*, Taylor & Francis. 12, 47–59. https://doi.org/10.1080/17452759.2016.1274490

[6] ASTM International. (2013) F2792-12a - Standard Terminology for Additive Manufacturing Technologies. *Rapid Manufacturing Association*, 10–2. https://doi.org/10.1520/F2792-12A

[7] Kramer, T.R., Proctor, F.M. and Messina, E. (2000) The NIST RS274NGC Interpreter. 121. https://doi.org/10.1.1.15.7813

[8] Bowyer, A. The RepRap project: G-code: RepRap Wiki [Internet].

[9] Levine, L. and Miller, R.C. (2007) 12 Extrusion Processes.

[10] Jones, R., Haufe, P., Sells, E., Iravani, P., Olliver, V., Palmer, C. et al. (2011) Reprap - The replicating rapid prototyper. *Robotica*, 29, 177–91. https://doi.org/10.1017/S026357471000069X

[11] Bellini, A., Güçeri, S. and Bertoldi, M. (2004) Liquefier Dynamics in Fused Deposition. *Journal of Manufacturing Science and Engineering*, 126, 237. https://doi.org/10.1115/1.1688377

[12] Gibson, I., Rosen, D. and Stucker, B. (2015) Extrusion-Based Systems. *Additive Manufacturing Technologies: Rapid Prototyping to Direct Digital Manufacturing*,. https://doi.org/10.1007/978-1-4939-2113-3

[13] Boparai, K.S. and Singh, R. (2017) Advances in Fused Deposition Modeling. *Materials Science and Materials Engineering*, 1–9. https://doi.org/10.1016/B978-0-12-803581-8.04166-7

[14] Ngo, T.D., Kashani, A., Imbalzano, G., Nguyen, K.T.Q. and Hui, D. (2018) Additive

manufacturing (3D printing): A review of materials, methods, applications and challenges. *Composites Part B: Engineering*, Elsevier. 143, 172–96. https://doi.org/10.1016/j.compositesb.2018.02.012

[15] Bourell, D., Kruth, J.P., Leu, M., Levy, G., Rosen, D., Beese, A.M. et al. (2017) Materials for additive manufacturing. *CIRP Annals - Manufacturing Technology*, CIRP. 66, 659–81. https://doi.org/10.1016/j.cirp.2017.05.009

[16] Gebhardt, A., Kessler, J. and Thurn, L. (2019) Materials and Design. In: Smith DM, editor. *3D Printing Understanding Additive Manufacturing*, Second. Munich, Germany. https://doi.org/10.1016/C2009-0-26530-5

[17] Kruth, J.P., Levy, G., Klocke, F. and Childs, T.H.C. (2007) Consolidation phenomena in laser and powder-bed based layered manufacturing. *CIRP Annals - Manufacturing Technology*, 56, 730–59. https://doi.org/10.1016/j.cirp.2007.10.004

[18] Wang, X., Jiang, M., Zhou, Z., Gou, J. and Hui, D. (2017) 3D printing of polymer matrix composites: A review and prospective. *Composites Part B: Engineering*, Elsevier Ltd. 110, 442–58. https://doi.org/10.1016/j.compositesb.2016.11.034

[19] Srivastava, V.K. (2017) A reviev on advances in rapid prototype 3D printing of multi-functional applications. *Science and Technology*, 7, 4–24. https://doi.org/10.5923/j.scit.20170701.02

[20] Masood, S.H. (2014) Advances in Fused Deposition Modeling [Internet]. Compr. Mater. Process. Elsevier. https://doi.org/10.1016/B978-0-08-096532-1.01002-5

[21] Fitzharris, E.R., Watanabe, N., Rosen, D.W. and Shofner, M.L. (2018) Effects of material properties on warpage in fused deposition modeling parts. *The International Journal of Advanced Manufacturing Technology*, The International Journal of Advanced Manufacturing Technology. 95, 2059–70. https://doi.org/10.1007/s00170-017-1340-8

[22] Kuo, C. (2019) Minimizing warpage of ABS prototypes built with low-cost fused deposition modeling machine using developed closed-chamber and optimal process parameters. *The International Journal of Advanced Manufacturing Technology*, The International Journal of Advanced Manufacturing Technology. 101, 593–602. https://doi.org/https://doi.org/10.1007/s00170-018-2969-7

[23] Liu, Z., Wang, Y., Wu, B., Cui, C., Guo, Y. and Yan, C. (2019) A critical review of fused deposition modeling 3D printing technology in manufacturing polylactic acid parts. *The International Journal of Advanced Manufacturing Technology*, The International Journal of Advanced Manufacturing Technology. 102, 2877–89. https://doi.org/https://doi.org/10.1007/s00170-019-03332-x

[24] Tanaka, K., Osuga, H., Suzuki, H., Shogase, Y. and Kitahara, Y. (1998) Synthesis , enzymic resolution and enantiomeric enhancement of bis (hydroxymethyl) [7] thiaheterohelicenes Kazuhiko Tanaka ,* Hideji Osuga , Hitomi Suzuki , Yuka Shogase and. 935–40.

[25] Singh, R., Kumar, R., Farina, I., Colangelo, F., Feo, L. and Fraternali, F. (2019) Multi-Material Additive Manufacturing of Sustainable Innovative Materials and Structures. 1–14.

https://doi.org/10.3390/polym11010062

[26] Generic Families of Plastic | UL Prospector [Internet].

[27] Gibson, I., Rosen, D.W. and Stucker, B. (2010) The use of multiple materials in additive manufacturing. *Additive Manufacturing Technologies: Rapid Prototyping to Direct Digital Manufacturing*, p. 423–36. https://doi.org/10.1007/978-1-4419-1120-9

[28] De Souza, A.M.C., Cucchiara, M.G. and Ereio, A.V. (2016) ABS/HIPS blends obtained from WEEE: Influence of processing conditions and composition. *Journal of Applied Polymer Science*, 133, 1–7. https://doi.org/10.1002/app.43831

[29] Singh, R., Singh, J. and Singh, S. (2016) Investigation for dimensional accuracy of AMC prepared by FDM assisted investment casting using nylon-6 waste based reinforced filament. *Measurement: Journal of the International Measurement Confederation*, Elsevier Ltd. 78, 253–9. https://doi.org/10.1016/j.measurement.2015.10.016

[30] Inamdar A, Magana M, Medina F, Grajeda Y, W.R. (2006) Development of an automated multiple material stereolitography machine. *Proceedings of 17th Annual Solid Freeform Fabrication Symposium*, Austin, Texas. p. 624–35.

[31] Moore, J.P. and Williams, C.B. (2015) Fatigue properties of parts printed by PolyJet material jetting. *Rapid Prototyping Journal*, 21, 675–85. https://doi.org/10.1108/RPJ-03-2014-0031

[32] Khalil, S., Nam, J. and Sun, W. (2004) Multi-Nozzle Biopolymer Deposition for Freeform Fabrication of Tissue Constructs. *Proceedings of 14th Interdisciplinary Research Conference on Biomaterials*, Limoges, France. p. 826–37. https://doi.org/10.1109/NEBC.2004.1300032

[33] Zhang, Z. and Joshi, S. (2017) Slice data representation and format for multi-material objects for additive manufacturing processes. *Rapid Prototyping Journal*, 23, 149–61. https://doi.org/10.1108/RPJ-04-2014-0047

[34] Jafari, M.A., Han, W., Mohammadi, F., Safari, A., Danforth, S.C. and Langrana, N. (2000) A novel system for fused deposition of advanced multiple ceramics. *Rapid Prototyping Journal*, 6, 161–74. https://doi.org/10.1108/13552540010337047

[35] Ali, M.H., Mir-Nasiri, N. and Ko, W.L. (2016) Multi-nozzle extrusion system for 3D printer and its control mechanism. *International Journal of Advanced Manufacturing Technology*, The International Journal of Advanced Manufacturing Technology. 86, 999–1010. https://doi.org/10.1007/s00170-015-8205-9

[36] Test, P., Average, A., Actual, D. and Accuracy, R. OpenBuilds Actuator Testing Data [Internet]. p. 1–7.

[37] Qin, Y., Qi, Q., Scott, P.J. and Jiang, X. (2019) Status, comparison, and future of the representations of additive manufacturing data. *CAD Computer Aided Design*, Elsevier Ltd. 111, 44–64. https://doi.org/10.1016/j.cad.2019.02.004

[38] Coasterman. (2011) The Essential Calibration Set - Thingiverse [Internet].

[39] Loohney. (2017) Basic Stringing Test - Thingiverse [Internet].

[40] Jain, P. and Kuthe, A.M. (2013) Feasibility study of manufacturing using rapid prototyping: FDM approach. *Procedia Engineering*, Elsevier B.V. 63, 4–11. https://doi.org/10.1016/j.proeng.2013.08.275

[41] Turner, B.N., Strong, R. and Gold, S.A. (2014) A review of melt extrusion additive manufacturing processes: I. Process design and modeling. *Rapid Prototyping Journal*, 20, 192–204. https://doi.org/10.1108/RPJ-01-2013-0012

[42] Mohamed, O.A., Masood, S.H. and Bhowmik, J.L. (2015) Optimization of fused deposition modeling process parameters: a review of current research and future prospects. *Advances in Manufacturing*, 3, 42–53. https://doi.org/10.1007/s40436-014-0097-7

[43] Messimer, S.L., Patterson, A.E., Muna, N., Deshpande, A.P. and Rocha Pereira, T. (2018) Characterization and Processing Behavior of Heated Aluminum-Polycarbonate Composite Build Plates for the FDM Additive Manufacturing Process. *Journal of Manufacturing and Materials Processing*, 2, 12. https://doi.org/10.3390/jmmp2010012

[44] Torrado, A.R., David, P. and Wicker, R.B. (2014) Fracture Surface Analysis of 3D-Printed Tensile Specimens of Novel ABS-Based Materials. *Journal of Failure Analysis and Prevention*, 14, 343–53. https://doi.org/10.1007/s11668-014-9803-9

[45] Rutkowski, J. V and Barbara, C. (1986) Pyrolysis and Combustion Products and their Toxicity-A Review of the Literature. *Fire and Materials*, 10, 93–105. https://doi.org/https://doi.org/10.1002/fam.810100303

[46] Kumar, R. and Singh, R. (2018) On the 3D printing of recycled ABS , PLA and HIPS thermoplastics for structural applications. *PSU Research Revieu*, 2, 115–37. https://doi.org/10.1108/PRR-07-2018-0018

[47] Lopes, L.R., Silva, A.F. and Carneiro, O.S. (2018) Multi-material 3D printing: The relevance of materials affinity on the boundary interface performance. *Additive Manufacturing*, 23, 45–52. https://doi.org/10.1016/j.addma.2018.06.027

[48] Song, H. and Lefebvre, S. (2017) Colored fused filament fabrication [Internet].

[49] Roger, F. (2015) 3D-printing of thermoplastic structures by FDM using heterogeneous infill and multi-materials : An integrated design-advanced manufacturing approach for factories of the future Abstract : *22ème Congrès Français de Mécanique*, Lyon, France. p. 1–7.

[50] Joseph Prusa. (2018) Multi Material - Prusa Printers [Internet].

[51] Espalin, D., Ramirez, J., Medina, F. and Wicker, R. (2012) Multi-Material, Multi-Technology FDM System. *Proceedings of the Solid Freeform FAbrication Symposium Workshop*, El Paso, Texas. p. 828–35.

[52] Yin, J., Lu, C., Fu, J., Huang, Y. and Zheng, Y. (2018) Interfacial bonding during multi-material fused deposition modeling (FDM) process due to inter-molecular diffusion. *Materials & Design*, Elsevier Ltd. 150, 104–12. https://doi.org/10.1016/j.matdes.2018.04.029

[53] ASTM International. (2003) Standard test method for tensile properties of plastics. *ASTM Internationai*, 8, 46–58. https://doi.org/10.1520/D0638-14.1

[54] Vaezi, M., Chianrabutra, S., Mellor, B. and Yang, S. (2013) Multiple material additive manufacturing - Part 1: A review: This review paper covers a decade of research on multiple material additive manufacturing technologies which can produce complex geometry parts with different materials. *Virtual and Physical Prototyping*, 8, 19–50. https://doi.org/10.1080/17452759.2013.778175

[55] E3D Kraken (2016) - Multi-Nozzled, Water-Cooled, Bowden-Fed Extrusion | E3D Online [Internet].

[56] RepRap.me (2015) [Internet]. Diam. Hotend.

[57] Hergel, J. and Lefebvre, S. (2014) Clean color: Improving multi-filament 3D prints. *Computer Graphics Forum*, 33, 469–78. https://doi.org/10.1111/cgf.12318

[58] Sanchez, A. and Comas, A.S. (2015) Application of Taguchi Experimental Design for identification of factors influences over 3D Printing Time. *IJMSOR*, 1, 43–8. https://doi.org/10.13140/RG.2.1.4529.8649

[59] Gibson, I., Rosen, D. and Stucker, B. (2015) Additive Manufacturing Technologies: 3D Printing, Rapid Prototyping, and Direct Digital Manufacturing [Internet]. https://doi.org/10.1007/978-1-4939-2113-3

[60] Liu, J., Ma, Y., Qureshi, A.J. and Ahmad, R. (2018) Light-weight shape and topology optimization with hybrid deposition path planning for FDM parts. *The International Journal of Advanced Manufacturing Technology*, 97, 1123–35. https://doi.org/10.1007/s00170-018-1955-4

[61] Thompson, M.K., Moroni, G., Vaneker, T., Fadel, G., Campbell, R.I., Gibson, I. et al. (2016) Design for Additive Manufacturing: Trends, opportunities, considerations, and constraints. *CIRP Annals - Manufacturing Technology*, CIRP. 65, 737–60. https://doi.org/10.1016/j.cirp.2016.05.004

[62] Strong, D., Kay, M., Conner, B., Wakefield, T. and Manogharan, G. (2018) Hybrid manufacturing – integrating traditional manufacturers with additive manufacturing (AM) supply chain. *Additive Manufacturing*, 21, 159–73. https://doi.org/10.1016/j.addma.2018.03.010

[63] Liu, J., Zheng, Y., Ma, Y., Qureshi, A. and Ahmad, R. (2019) A Topology Optimization Method for Hybrid Subtractive–Additive Remanufacturing. *International Journal of Precision Engineering and Manufacturing-Green Technology*, Korean Society for Precision Engineering. https://doi.org/10.1007/s40684-019-00075-8

[64] Dilberoglu, U.M., Gharehpapagh, B., Yaman, U. and Dolen, M. (2017) The Role of Additive Manufacturing in the Era of Industry 4.0. *Procedia Manufacturing*, The Author(s). 11, 545–54. https://doi.org/10.1016/j.promfg.2017.07.148

[65] Alghamdy, M., Ahmad, R. and Alsayyed, B. (2019) Material Selection Methodology for Additive Manufacturing Applications. *Procedia CIRP*, Elsevier B.V. 84, 486–90. https://doi.org/10.1016/j.procir.2019.04.265

[66] Yang, Y., Chen, Y., Wei, Y. and Li, Y. (2016) 3D printing of shape memory polymer for

functional part fabrication. *International Journal of Advanced Manufacturing Technology*, The International Journal of Advanced Manufacturing Technology. 84, 2079–95. https://doi.org/10.1007/s00170-015-7843-2

[67] Biron, M. (2013) Plastics Solutions for Practical Problems. *Thermoplastics and Thermoplastic Composites*, p. 883–1038. https://doi.org/10.1016/b978-1-4557-7898-0.00007-x

[68] Kaw, A.K. and Group, F. (2006) Failure, Analysis, and Design of Laminates. *Mechanics of Composite Materials*, Second Ed. p. 419–25.

[69] We, H. (2000) Sandwich structures. *Metal Foams*, p. 113–49. https://doi.org/10.1016/B978-075067219-1/50012-X

[70] Daniel, I.M. and Abot, J.L. (2000) Fabrication, testing and analysis of composite sandwich beams. *Composites Science and Technology*, 60, 2455–63. https://doi.org/10.1016/S0266-3538(00)00039-7

[71] Herranen, H., Pabut, O., Eerme, M., Majak, J., Pohlak, M., Kers, J. et al. (2012) Design and testing of sandwich structures with different core materials. *Medziagotyra*, 18, 45–50. https://doi.org/10.5755/j01.ms.18.1.1340

[72] Lanzotti, A., Grasso, M., Staiano, G. and Martorelli, M. (2015) The impact of process parameters on mechanical properties of parts fabricated in PLA with an open-source 3-D printer. *Rapid Prototyping Journal*, 21, 604–17. https://doi.org/10.1108/RPJ-09-2014-0135

[73] Chacón, J.M., Caminero, M.A., García-Plaza, E. and Núñez, P.J. (2017) Additive manufacturing of PLA structures using fused deposition modelling: Effect of process parameters on mechanical properties and their optimal selection. *Materials and Design*, Elsevier Ltd. 124, 143–57. https://doi.org/10.1016/j.matdes.2017.03.065

[74] Fernandez-Vicente, M., Calle, W., Ferrandiz, S. and Conejero, A. (2016) Effect of Infill Parameters on Tensile Mechanical Behavior in Desktop 3D Printing. *3D Printing and Additive Manufacturing*, 3, 183–92. https://doi.org/10.1089/3dp.2015.0036

[75] Qureshi, A.J., Mahmood, S., Wong, W.L.E. and Talamona, D. (2015) Design for scalability and strength optimisation for components created through fdm process. *Proceedings of the International Conference on Engineering Design, ICED*, 6, 255–66.

[76] Kim, H., Park, E., Kim, S., Park, B., Kim, N. and Lee, S. (2017) Experimental Study on Mechanical Properties of Single- and Dual-material 3D Printed Products. *Procedia Manufacturing*, The Author(s). 10, 887–97. https://doi.org/10.1016/j.promfg.2017.07.076

[77] Saad, N.A. and Sabah, A. (2016) An Investigation of New Design of Light Weight Structure of (ABS / PLA) by Using of Three Dimensions Printing. *13th International Conference "Standardization, Prototypes and Quality: A Means of Balkan Countries' Collaboration,"* Brasov, Romania. p. 482–7.

[78] Brischetto, S., Ferro, C.G., Torre, R. and Maggiore, P. (2018) 3D FDM production and mechanical behavior of polymeric sandwich specimens embedding classical and honeycomb cores. *Curved and Layered Structures*, 5, 80–94. https://doi.org/10.1515/cls-2018-0007

[79] Santosh, R.V.N., Sarojini, J., Vikram, K.A. and Lakshmi, V.V.K. (2019) Evaluating the Mechanical Properties of Commonly Used 3d Printed ABS and PLA Polymers with Multi Layered Polymers. *International Journal of Engineering and Advanced Technology*, 8, 2351–6. https://doi.org/10.35940/ijeat.f8646.088619

[80] Dinesh, S., Rajasekaran, T., Dhanasekaran, M. and Vigneshwaran, K. (2018) Experimental testing on mechanical properties of sandwich structured carbon fibers reinforced composites. *IOP Conference Series: Materials Science and Engineering*, 402, 12180. https://doi.org/10.1088/1757-899x/402/1/012180

[81] Galatas, A., Hassanin, H., Zweiri, Y. and Seneviratne, L. (2018) Additive manufactured sandwich composite/ABS parts for unmanned aerial vehicle applications. *Polymers*, 10, 1262. https://doi.org/10.3390/polym10111262

[82] Wittbrodt, B. and Pearce, J.M. (2015) The effects of PLA color on material properties of 3-D printed components. *Additive Manufacturing*, 8, 110–6. https://doi.org/10.1016/j.addma.2015.09.006